HHS Public Access

Author manuscript

Comp Biochem Physiol B Biochem Mol Biol. Author manuscript; available in PMC 2023 June 28.

Published in final edited form as:

Comp Biochem Physiol B Biochem Mol Biol. 2022 ; 262: 110777. doi:10.1016/j.cbpb.2022.110777.

Gene expression and functional analysis of Aha1a and Aha1b in stress response in zebrafish

Huanhuan Xiao[1], **Hongying Wang**[1,2], **Qiuxia He**[1,3], **Jianfeng Zhou**[1,4], **Shaojun Du**[1,*]

[1]Institute of Marine and Environmental Technology, Department of Biochemistry and Molecular Biology, University of Maryland School of Medicine, Baltimore, MD 21202, USA

[2]College of Life Science, South-Central Minzu University, Wuhan 430074, China

[3]Science and Technology Service Platform of Shandong Academy of Sciences, Qilu University of Technology, Shandong Academy of Sciences, Jinan, China

[4]School of Medicine and Pharmacy, Ocean University of China, Qingdao 266003, China

Abstract

Activator of heat shock protein 90 (hsp90) ATPase (Aha1) is a Hsp90 co-chaperone required for Hsp90 ATPase activation. Aha1 is essential for yeast survival and muscle development in *C. elegans* under elevated temperature and hsp90-deficeiency induced stress conditions. The roles of Aha1 in vertebrates are poorly understood. Here, we characterized the expression and function of Aha1 in zebrafish. We showed that zebrafish genome contains two *aha1* genes, *aha1a* and *aha1b*, that show distinct patterns of expression during development. Under normal the physiological condition, *aha1a* is primarily expressed in skeletal muscle cells of zebrafish embryos, while *aha1b* is strongly expressed in the head region. *aha1a* and *aha1b* expression increased dramatically in response to heat shock induced stress. In addition, Aha1a-GFP fusion protein exhibited a dynamic translocation in muscle cells in response to heat shock. Moreover, upregulation of *aha1* expression was also observed in *hsp90a1* knockdown embryos that showed a muscle defect. Genetic studies demonstrated that knockout of *aha1a, aha1b* or both had no detectable effect on embryonic development, survival, and growth in zebrafish. The *aha1a* and *aha1b* mutant embryos showed normal muscle development and stress response in response to heat shock. Single or double *aha1a* and *aha1b* mutants could grow into normal reproductive adults with normal skeletal muscle structure and morphology compared with wild type control. Together, data from these studies indicate that Aha1a and Aha1b are involved in stress response. However, they are dispensable in zebrafish embryonic development, growth, and survival.

[*]Corresponding Author: Dr. Shaojun Du, Institute of Marine and Environmental Technology, Department of Biochemistry and Molecular Biology, University of Maryland School of Medicine, 701 East Pratt Street, Baltimore, MD 21202, USA, Tel: 410-234-8854, Fax: 410-234-8896, sdu@som.umaryland.edu.

Author contributions SD conceived the project. HX cloned the *aha1a* and *aha1b* genes from zebrafish and generated the *p(ef1α:Aha1a-GFP)* and *p(ef1α:Aha1b-GFP)* constructs. XH, HW, QH and JZ generated the *aha1a* and *aha1b* mutants using TALEN and CRISPR. HX performed the subcellular localization and functional studies. HX wrote the first draft and prepared figures for the manuscript. All authors contributed to the data analysis. SD revised the manuscript.

Disclosures: The authors have no conflicts of interest to disclose.

Keywords

Heat shock response; Aha1(activator of Hsp90 ATPase); heat shock protein; myosin chaperone

Introduction

Heat shock protein 90s (Hsp90s) are evolutionarily conserved molecular chaperones that exist in almost all kingdoms except for archaea (Chen, 2006; Hendrick and Hartl, 1993; Wang et al., 2004). Hsp90 proteins serve as key regulators of proteostasis under both physiological and stress conditions (Geller et al., 2018; Hoter et al., 2018; Schopf et al., 2017; Taipale et al., 2010). They play critical roles in protein folding, maturation, and function (Buchberger et al., 2010; Vabulas et al., 2010). In addition, Hsp90s are also involved in denatured protein degradation to prevent protein aggregation, thus are vital components for maintenance of cellular homeostasis (Benjamin and McMillan, 1998; Geller et al., 2018; Lackie et al., 2017).

Genetic studies in yeast, *C. elegans* and *Drosophila* demonstrated that Hsp90s are essential for their longevity and viability (Borkovich et al., 1989; Picard et al., 1990). In *C. elegans*, DAF-21/Hsp90 is required for C. elegans longevity (Somogyvári et al., 2018). Null mutation of daf-21 gene (hsp-90 homolog) causes muscle defects and early larval lethal (Gaiser et al., 2011). In *Drosophila*, Hsp83 (Hsp90 ortholog) is required for the development of many different morphological structures (Rutherford and Lindquist, 1998). And mutant Hsp83 alleles are embryonic lethal (Cutforth and Rubin, 1994; van der Straten et al., 1997; Yue et al., 1999).

Vertebrates have two cytosolic Hsp90 proteins, Hsp90α and Hsp90β that show different functions and response to stress. Hsp90α is induced upon stress conditions, while Hsp90β is constitutively expressed (Hoter et al., 2018; Sreedhar et al., 2004). Hsp90α and Hsp90β have different functions in animal development and viability. Hsp90β knock-out mice are embryonic lethal around E9/9.5 due to defective allantois and allantois-trophoblast interaction (Voss et al., 2000). In contrast, loss of Hsp90α has no effect on mouse survival. The Hsp90α mutant mice showed defective spermatogenesis and spermatocyte survival (Grad et al., 2010; Kajiwara et al., 2012), antigen cross-presentation (Ichiyanagi et al., 2010; Imai et al., 2011), reduced myocardial fibrosis (Cáceres et al., 2018; García et al., 2016), and retinitis pigmentosa (Wu et al., 2020). Genetic analysis in zebrafish revealed that Hsp90α1 is essential for myosin folding and sarcomere assembly in skeletal muscles (Du et al., 2008; Etard et al., 2007; Hawkins et al., 2008).

Hsp90s are dimeric molecular chaperones that function in an ATP-dependent activation cycle. The Hsp90 dimer undergoes a series of structural rearrangements during its ATPase cycle (Li et al., 2012; Li and Buchner, 2013). In the nucleotide-free form, the dimerized Hsp90 chaperones adopts an open conformation, which closes upon ATP hydrolysis, a process that promotes protein folding (Prodromou et al., 2000). A cohort of accessory proteins called ‘co-chaperones’ play critical roles in the Hsp90 chaperone cycle by participating in client recruitment, Hsp90 ATPase activity and conformational rearrangement (Biebl and Buchner, 2019; Pratt and Toft, 2003; Zuehlke and Johnson, 2010). More than 20

co-chaperones have been identified in eukaryotic cells that are involved in regulating Hsp90 function (Bhattacharya et al., 2020; Biebl et al., 2020; Chen et al, 1998; Li et al., 2011; Roe et al, 2004; Sahasrabudhe et al., 2017). The co-chaperone Aha1 is one of the most prominent activators of Hsp90 (Panaretou et al., 2002). Aha1 binds to the Hsp90 middle domain and exerts stimulatory effect on Hsp90 ATPase activity (Armstrong et al., 2012; Lotz et al., 2003; Horvat et al., 2014; Meyer et al., 2004; Retzlaff et al., 2010; Wolmarans et al., 2016).

Aha1 is found in all eukaryotic cells, from yeast to human. Genetic analysis revealed that Aha1 is not essential for Hsp90 function and yeast survival under normal condition (Panaretou et al., 2002). However, yeast strains with Aha1 deletions showed compromised Hsp90 function and survival in elevated temperatures (Panaretou et al., 2002). Similarly, knockdown of Aha1 (ahsa-1) expression in *Caenorhabditis elegans* had no apparent phenotype under normal condition. However, under stress conditions from *unc*-45 temperature-sensitive mutation and Hsp90 deficiency, Aha1 (ahsa-1) was found to be required for muscle homeostasis and integrity (Frumkin et al., 2014). A recent study demonstrated that overexpression of Aha1 promotes tau pathogenesis in aged mice (Criado-Marrero et al., 2021). Downregulation of Aha1 rescues misfolding of CFTR in cystic fibrosis (Wang et al., 2006). Genetic studies in zebrafish via overexpression and knockdown revealed a role for Aha1 in mediating the variability of craniofacial defects in GATA3 mutant fish embryos (Sheehan-Rooney et al., 2013). All these studies were performed by using overexpression or knockdown approaches, no vertebrate animal models have been generated with null Aha1 mutations, and thus the roles of Aha1 in the development of vertebrate growth and survival are largely unknown.

The aim of this study is to investigate the expression and function of Aha1 in zebrafish. We showed that zebrafish *aha1a* and *aha1b* genes have distinct patterns of expression. Under normal physiological conditions, *aha1a* is primarily expressed in skeletal muscles of zebrafish embryos, while *aha1b* is strongly expressed in the head region. In response to heat shock, *aha1a* and *aha1b* showed a dramatic upregulation of expression in skeletal muscles and in the whole body, respectively. In addition, disruption of muscle development from knockdown of *hsp90α1* also resulted in muscle-specific upregulation of *aha1a and aha1b* expression in fish embryos. However, knockdown of *hsp90α2* without a muscle defect had no effect on *aha1a and aha1b* expression in developing muscle of zebrafish embryos. Moreover, knockout of *aha1a* or *aha1b* in zebrafish had no detectable effect on embryonic development and fish survival. Collectively, our studies indicate that Aha1a and Aha1b are involved in stress response, but they are dispensable in fish embryonic development and survival.

Materials and methods

Ethics statement

This study was carried out according to Guide for the Care and Use of Laboratory Animals of the National Institutes of Health. Fish embryos over 24 hours-post-fertilization (hpf) were anaesthetized in 0.6 mM Tricaine (pH 7.0) before fixation in 4% paraformaldehyde (PFA) for immunostaining and whole mount in-situ hybridization. The protocol was approved by

the Institutional Animal Care and Use Committee of University of Maryland Baltimore (Permit Number: 0516005).

Zebrafish lines and maintenance

Adult zebrafish were raised at the zebrafish facility at the Institute of Marine and Environmental Technology, University of Maryland. Zebrafish were kept at 28.5°C in a recirculating aquatic system at a photoperiod of 14/10 hour light/dark cycle in aquaria supplied with freshwater and aeration. The *myom3*^{mnGt0067} zebrafish line was obtained from Steve Ekker's laboratory at the Mayo Clinic (USA) which carried an insertion of red florescent protein gene (RFP) in the *myomesin-3* (*myom3*) gene (Clark et al., 2011; Xu et al., 2012). Myomesin-3-RFP specifically labels M-lines in the sarcomeres. The *aha1a and aha1b* single and double mutant alleles were generated in our laboratory.

Generation of TALEN targeted to Aha1a

Mojo Hand (www.talendesign.org) was used to find candidate TALEN binding sites for Aha1a. Three criteria were used for TALEN design. First, TALEN binding sites were selected that ranged from 15 to 18 bases in length. Second, the spacer length was initially selected to be 15 to 16 base pairs (bps). Additionally, when possible, TALEN target sequences were selected with a restriction enzyme centrally located in the spacer. DNA sequences of the Tal1 and Tal2 target sites and restriction enzyme cutting site in the spacer were listed in Table 1 (Supplemental material).

TALEN assembly of the 15 RVD-containing repeats was conducted according to the method described by Cermak and colleagues (Cermak et al., 2011). The RVDs 1–10 were cloned into pFUS_A and the RVDs 11–14 were cloned into pFUS_B. The resulting pFUS_A and pFUS_B of TAL1 were cloned into pCS2TAL3_DD vector which contains the last RVD of TAL1. Similarly, pFUS_A and pFUS_B of TAL2 were cloned into pCS2TAL3_RR vector which contains the last RVD of TAL2. TAL1 and Tal2 mRNAs were synthesized by in vitro transcription using the SP6 mMESSAGE mMACHINE Kit (Ambion).

Synthesis of aha1a and aha1b targeting sgRNAs

sgRNA target sequences were identified using the program at http://zifit.partners.org/ZiFiT/CSquare9Nuclease.aspx. Two sgRNA target sequences (*aha1a-sg*RNA-4 and *aha1a*-sgRNA-6) were identified in the exon 5 and exon 7 of the *aha1a* gene, whereas one *aha1b-sg*RNA-3 target sequence was identified in the exon 2 of zebrafish *aha1b* gene. DNA templates for synthesizing *aha1a* and *aha1b* sgRNAs were generated by PCR using pDR274 vector as a template (Hwang et al., 2013). The PCR was carried out using the Phusion DNA polymerase (ThermoFisher) with *aha1a* or *aha1b* specific forward primers and a common reverse primer (Cas9-P4) (Table 2). *aha1a* and *aha1b-sg*RNAs were synthesized in *vitro* by using the MEGA shortscript T7 Kit (Thermo Fisher AM1354). The sgRNA transcripts were purified using MEGAclear Transcription Clean-Up Kit (Thermo Fisher).

Construction of pTol2(ef1a:Aha1a-GFP) and pTol2(ef1a:Aha1b-GFP) plasmids

DNA constructs, pTol2(ef1α:Aha1a-GFP) and pTol2(ef1α:Aha1b-GFP), expressing the Aha1a-GFP or Aha1b-GFP fusion proteins were generated. Briefly, full-length Aha1a and

Aha1b coding sequence without the stop codon were generated by PCR using Pfu Turbo DNA polymerase (Agilent) using Aha1a-GFP-EF2/ER or Aha1b-GFP-EF2/ER in-fusion primers (Table 2, Supplemental material). The PCR products of Aha1a and Aha1b was cloned into the BamHI site of pTol2 vector (Urasaki et al., 2006) using the In-Fusion Cloning Kit (Takara Bio USA, Inc). The Aha1a and Aha1b coding sequences were cloned in-frame upstream of the EGFP coding sequence in the pTol2 vector. The DNA sequences of pTol2(ef1α:Aha1a-GFP) and pTol2(ef1α:Aha1b-GFP) plasmids were confirmed by Sanger sequencing. Aha1a-GFP and Aha1a-GFP expression was directed by the *Xenopus* elongation factor 1α (ef1α) gene enhancer–promoter (Johnson and Krieg, 1994).

Microinjection in zebrafish embryos

Morpholino antisense oligos were synthesized by Gene Tools (Carvalis, OR). The Hsp90α1-MO and Hsp90α2-MO translation blockers were targeted to sequence near the ATG start codon (Du et al., 2008). The standard control MO (Con-MO) from Gene Tools was used as the negative control. Morpholino antisense oligos were dissolved in 1x Danieau buffer to a final concentration of 0.25 mM (Nasevicius and Ekker, 2000). Approximately 1–2 nl (2.5–5 ng) were injected into each zebrafish embryo at the 1 or 2 cell stages.

For the TALEN approach, a pair of two TALENs (TAL1 and TAL2) mRNAs was co-injected into one-cell stage wild type zebrafish embryos. Each embryo was injected with 2 nl of solution containing about 50ng/μl of TALE mRNA. To knock out genes using CRISPR, gene-specific sgRNAs were mixed with equal volume of Cas9 protein (B25640, ThermoFisher) and co-injected into wildtype zebrafish embryos at 1–2 cell stages. The final concentrations of the mixed sgRNAs and Cas9 protein were 25 ng/μl and 250 ng/μl, respectively. Each embryo was injected with approximately 2 nl of the mixed solution containing approximately 60 pg sgRNA and 500 pg of Cas9 protein.

DNA isolation and genotyping of F0 injected embryos by DNA sequencing

Genomic DNAs were extracted from injected embryo at 48 hpf using the alkaline method (Cai et al., 2018). Genomic DNAs from randomly selected ten embryos for each group were subjected to sequencing using the forward and reverse primers for each *sg*RNA of *aha1a* and *aha1b* (Table 2). Mutant alleles were identified by the presence of mixed population of sequences compared to respective uniform DNA sequence from the wild-type embryos,

Genotyping F1, F2 and F3 fish using DNA from caudal fin clips

To genotype adult zebrafish at the F1 and following generations, caudal fin was cut from individual zebrafish. DNA was extracted from the fin clip using the alkaline method (Cai et al., 2018). The PCR reaction was carried out in a 15 μl reaction using GoTaq® DNA polymerase (Promega). DNA sequences at the *aha1a* and *aha1b* target sites were amplified using respective gene specific primers (Table 2, Supplemental material). The *aha1a*$^{+17}$ allele targeted by aha1a-sgRNA4 was amplified using aha1a-sgRNAx3/4-F and aha1a-sgRNAx3/4-R primers. The PCR products of *aha1a*$^{+17}$ was digested with Hae III restriction enzyme. The Hae III site was abolished in the *aha1a*$^{+17}$ mutant containing a 17 bp insertion at the aha1a-sgRNA4 target site. The *aha1a*$^{-20}$ mutant allele generated by *aha1a-sgRNA-6* was amplified using sgRNAx5/6-F and sgRNAx5/6-R primers. The

aha1a^{-20} mutant alleles containing a 20 bp deletion that was detected on a 2.5% agarose gel and confirmed by DNA sequencing. The *aha1b*$^{-1}$ mutant allele was amplified with aha1b-sgRNA234-F2 and aha1b-sgRNA234-R2 primers. The PCR products of *aha1b* was digested with *Bfua*I restriction enzyme. The *Bfua*I site is in the *aha1b*$^{-1}$ mutant zebrafish containing a 1 bp deletion, but no *Bfua*I site in WT, thus simplifying the mutant screening and genotyping. For genotyping of *aha1b*$^{-4}$ (4 bp deletion) mutant, we designed two sets of primers (Table 2, Supplemental material). One pair of primers (Fw/m and Rw) specially amplified WT sequence at the aha1b-sgRNA4 target site. Another set of pairs (Fw/m and Rm) specifically amplified the mutant sequence with the 4 bp deletion. Both WT and *aha1b* mutant primers can amplify the heterozygous mutants (Table 2, Supplemental material). To sequence the PCR products, the PCR products were treated with ExoSAP-IT (USB) and sequenced directly using the PCR Fw/m forward primer.

Whole-mount phalloidin and immunostaining and in situ hybridization

Sarcomere organization was analyzed by antibody and phalloidin staining in zebrafish embryos as previously described (Tan et al., 2006; Cai et al., 2019; Jiao et al., 2021). Zebrafish embryos were fixed in 4% paraformaldehyde for 1 hr at room temperature. Immunostaining of myosin thick filaments and α-actinin at the Z-lines was caried out on the fixed embryos using anti-myosin F59 antibody and anti-α-actinin antibody, respectively. Staining of actin thin filaments was performed by incubating the embryos with 200ng/ml Phalloidin-TRITC (Sigma) for 60 min at room temperature in the dark. After immuno- or phalloidin-staining, the embryos were washed with PBST three times (30 min each). The trunk region of the embryos was dissected and mounted in Vectashied (Vector lab) for observation and photographing using a Leica SP8 confocal microscope.

Whole mount *in situ* hybridization was carried out using digoxigenin-labeled RNA antisense probes as previously described (Thisse et al., 2008). The DNA template for *aha1a* probe synthesis was generated by PCR using Aha1a-probe-2F/2R-T7 primers, whereas the DNA template for *aha1b* probe was generated by PCR using a pair of aha1b-probe-2F/2R-T7 primers, respectively (Table 2). DNA template for synthesis of *hsp90a1*, *hsp90a2* and *hsp90β* antisense probe was generated by PCR using a pair of hsp90α1-probe-F/P4R(T7), hsp90α2-probe-F/P5R(T7), and hsp90β-probe-F/R-T7 primers, respectively (Table 2, Supplemental material). Digoxigenin-labeled antisense probes were generated by *in vitro* transcription using MAXIscript T7 kit (AM1314M, Thermo Fisher). The images were acquired using a Leica dissecting microscope M12 equipped with a cool CCD digital camera (DX8, Olympus).

Regular and Real-Time RT-PCR analysis

Total RNA was extracted from wild type zebrafish embryos at various developmental stages from fertilization to 6 dpf and adult tissues using TRIzol Reagent (Life Technologies, Carlsbad, CA). In addition, total RNA was isolated from various types *aha1a* and *aha1b* mutant embryos at 24 and 48 hpf. cDNAs were generated using First-Strand cDNA synthesis kit (ThermoFisher Scientific, K1621). Genomic DNA was eliminated by DNase I digestion. The cDNAs were used as templates for PCR reaction. Primers for qPCR were designed

at the junctions of two adjacent exons to eliminate potential problems with genomic DNA contamination (Table 2, Supplemental material).

For real time PCR analysis, five 10-fold serial dilutions were applied to produce the standard curves of cDNA samples (Fig. S1, Supplemental material). PCR reaction was carried out using the standard SYBR Green PCR Mater Mix (Applied Biosystems) with 1 μl of 100× diluted cDNA template on a 7500 Fast Real-Time PCR System (Applied Biosystems). Each sample was performed in triplicate for PCR. Elongation factor 1α (ef-1α) was used as an internal reference gene. The 2−△△CT method was calculated to determine the relative levels of gene expression using the *ef-1α* for normalization. All results were expressed as mean ± SEM. Differences between WT and mutants were analyzed using a Student's t test, with a P value of <.05 as the level of significance.

Body weight and single fiber analysis

To compare fish body weight, three families of fish were generated by in-crossing of single or double mutants including *aha1a*$^{+17/+}$, *aha1b*$^{-4/+}$, or *aha1a*$^{+17/+}$;*aha1b*$^{-4}$. At 10-month-old, 54 adult fish were randomly selected from each of these 3 families for genotyping and body weight measurement.

For single fiber analysis, myofibers were dissected under microscope after digesting adult fish muscle tissue with 5mg/ml collagenase for 1–2 hrs. Single fiber isolation was performed as described (Roy et al., 2001; Ganassi et al., 2018; 2021; Shi et al., 2018). The dissected myofibers were placed on a slide and fixed for 15 min in 4% PFA and permeabilized with 0.5% Triton X-100 for 10 min. The fibers were stained with 30 ng/ml of phalloidin-TRITC conjugate (P1951, Sigma) and 1 μg/ml of Hoechst 32258. The fibers were mounted in VECTASHIELD mounting medium (Vector Labs, H-1000) and photographed using a Leica SP8 confocal microscope. All experiments were performed with at least three independent replicates. Student's t-test were performed among different groups. *P<0.05, **P<0.01 and ***P<0.001 were considered statistically significant. The experimental data obtained in this study were conducted by using the software Graphpad Prism.

Results

1. Zebrafish genome contains two *aha1* genes

Zebrafish *aha1* genes were identified and characterized. Sequence analysis revealed that zebrafish genome contains two *aha1* genes, *aha1a* and *aha1b*, located on chromosome 20 and 17, respectively. Phylogenetic analysis showed that in vertebrate groups, there are three main clades including fish Aha1a and Aha1b, mammalian Ahsa1(Aha1) and Ahsa2 (Aha2) (Fig. 1). Among them, zebrafish Aha1a and Aha1b are more closely related to mammalian Ahsa1 rather than Ahsa2 (Fig.1). Ahsa2 has been identified in mouse, pig and human genomes, and has yet to be identified in non-mammalian species. The two duplicated *aha1*genes, *aha1a* and *aha1b*, are unique to fish species. In lower eukaryotes, such as yeast, *C. elegans*, and *Drosophila*, only one *aha1* gene was identified in their genomes although a shorter homolog with sequence similarity to the N-terminus of Aha1 has been identified in yeast (Hch1) (Panaretou et al., 2002).

2. *aha1a* and *aha1b* show distinct patterns of expression in zebrafish embryos and adult tissue

The expression of *aha1a* and *aha1b* was analyzed by RT-PCR and whole mount *in situ* hybridization. RT-PCR showed that only weak *aha1a* expression was detected prior to 5 hours-post-fertilization (hpf) (Fig. 2A), while the expression of *aha1b* was throughout early embryogenesis from fertilization up to 6 days-post-fertilization (dpf) analyzed (Fig. 2A). The expression of *aha1a* expression increased significantly around 8 hpf, and a strong expression was maintained up to 6 dpf analyzed (Fig. 2A). Moreover, whole mount *in situ* hybridization showed that *aha1a* expression was primarily restricted to developing somites and skeletal muscles of fish embryos (Fig. 2B–F), whereas *aha1b* expression appeared to be much broader with a stronger signal in the head region and otic vesicles (Fig. 2G–K). In adult tissues, both *aha1a* and *aha1b* were expressed in all tissues analyzed including skeletal muscle, heart, gill, gut, eyes, liver, testes, ovaries, and brain (Fig. 2L). Collectively, these data indicate that although *aha1a* and *aha1b* have different patterns of expression during early development with *aha1a* expression primarily restricted to developing muscles and *aha1b* mainly in the head region, both genes show a broader pattern of expression in adult tissues.

3. *aha1a* and *aha1b* expression in stress response

Upregulation of chaperone gene expression is a typical response to heat shock and other stressing factors. Previous studies have shown that heat shock resulted in a strong upregulation of *hsp90* expression in zebrafish embryos (Krone et al., 1997; 2003; Li et al., 2013; Etard et al., 2015; Cai et al, 2019). To determine whether expression of *aha1a* and *aha1b* are responsive to stress, we analyzed their expression in zebrafish embryos subjected to 1h-heat shock treatment (37°C) at 24 or 48 hpf. The data showed that *aha1a* and *aha1b* expression was dramatically upregulated in heat shock treated fish embryos (Fig. 3B, D, F, H, J, I, N, P). Interestingly, *aha1a* and *aha1b* exhibited distinct patterns of upregulation. Compared with the untreated controls (Fig. 3A, E, I, M), upregulation of *aha1a* expression was mainly detected in skeletal muscle of the heat shock stressed embryos (Fig. 3B, F, D and H), whereas a global upregulation of *aha1b* expression was observed in the entire embryo at 24 hpf (Fig. 3J, N). However, the increased *aha1b* expression was mainly observed in the head region and pectoral fin bud of the heat shock treated embryos at 48 hpf (Fig. 3L, P). These data indicate that Aha1a and Aha1b are likely involved in stress response with a temporospatial regulated patterns.

Given that Aha1 is a Hsp90 cochaperone, we decided to test whether loss of Hsp90 could alter *aha1a* and *aha1b* expression. Gene specific antisense morpholino (MO) against *hsp90α1* or *hsp90α2* was injected into zebrafish embryos. Expression of *aha1a* and *aha1b* was determined by whole mount *in situ* hybridization in the injected embryos (Fig. 4). Compared with the control embryos (Fig. 4A, D, G and J), an upregulation of *aha1a* and *aha1b* expression was observed in trunk skeletal muscle of *hsp90α1* knockdown embryos (Fig. 4B, E, H and K). In contrast, no significant difference was detected in *hsp90α2* knockdown embryos (Fig. 4C, F, I and L). qRT-PCR analysis further confirmed the data from the whole mount *in situ* hybridization (Fig. 4H, I). Considering that *aha1a* is normally expressed in developing muscles of the zebrafish embryos, these data indicate that Aha1a

might be involved in Hsp90α1 function in muscle cell differentiation under both normal and stress conditions, while Aha1b might be only involved under stress conditions in muscle cells.

4. Aha1a showed a subcellular translocation in embryonic muscle fibers in response to heat shock

Stress can induce chaperone subcellular translocation. Previous studies demonstrated that Hsp90α protein displayed a dynamic translocation in zebrafish muscle cells in response to stress (Etard et al., 2008). To characterize Aha1a and Aha1b protein localization and determine whether their localization was affected by stress, we generated two DNA constructs expressing Aha1a-GFP and Aha1b-GFP fusion proteins, respectively. The DNA constructs were microinjected into zebrafish embryos for transient expression analysis. Aha1a-GFP and Aha1b-GFP protein localization were determined in muscle cells of injected zebrafish embryos at 48 hpf. Under normal physiological condition, most Aha1a-GFP and Aha1b-GFP displayed a sarcomeric pattern of localization between the M-lines marked with Myomesin-3-RFP (Fig. 5A–F), suggesting that they were likely localized at the Z-lines. This was confirmed by the Z-line specific with anti-α-actinin immunostaining (Data not shown). To assess whether Aha1b-GFP and Aha1b-GFP protein localization could be altered by stress, the injected embryos were subjected to heat shock treatment at 48 hpf. Aha1a-GFP and Aha1b-GFP localization was determined at 2 hrs after the heat shock treatment. The results showed a clear translocation of Aha1a-GFP from Z-lines to myosin enriched A-bands in myofibers of the heat shock treated embryos (Fig. 5G–I). In contrast, Aha1b-GFP did not display such translocation from Z-line to A-bands (Fig. 5J–L). Together, these data indicate that the Aha1a might be involved in heat shock response by re-locating to myosin rich A-bands to facilitate myosin folding and sarcomere assembly.

5. Loss of Aha1a and Aha1b had no effect on muscle development

To assess Aha1a and Aha1b function in muscle development, we generated zebrafish mutants carrying indel mutations in *aha1a* and *aha1b* genes using TALEN and CRISPR/Cas9 technologies Three mutant alleles, *aha1a*$^{-4}$, *aha1a*$^{+13}$ and *aha1a*$^{+20}$, were initially generated for *aha1a* using the TALEN technology targeted to exon 1 (Fig. S2, Supplemental material). The *aha1a*$^{-4}$, *aha1a*$^{+13}$ and *aha1a*$^{+20}$ mutant alleles carried a 4 bp deletion, 13 bp or 20 bp insertion, respectively (Fig. S2, Supplemental material). Bioinformatic analysis revealed that *aha1a* encodes two distinct mRNA transcripts that differ in the position of their ATG start codons in exon 1. Sequence analysis revealed that the three TALEN induced *aha1a*$^{-4}$, *aha1a*$^{+13}$ and *aha1a*$^{+20}$ mutants contained indels at position 49, 50 and 50 bp downstream of the first ATG start codon but before the second ATG start codon, raising questions of whether these mutants are completely null alleles.

To avoid the complexity from the second ATG start codon in *aha1a*$^{-4}$, *aha1a*$^{+13}$ and *aha1a*$^{+20}$ mutant alleles produced by TALEN, we decided to generate new *aha1a* mutant alleles using CRISPR targeted to exon 5 and exon 7. Two mutant alleles were generated for *aha1a*, named *aha1a*$^{+17}$ and *aha1a*$^{-20}$ (Fig. 6A, B). The *aha1a*$^{+17}$ and *aha1a*$^{-20}$ mutant alleles carried a 17 bp insertion and a 20 bp deletion in *aha1a* gene, respectively (Fig. S3, Supplemental material). Using CRISPR, we also generated two *aha1b* mutant alleles,

namely *aha1b*$^{-4}$ and *aha1b*$^{-1}$ (Fig. 6C). The *aha1b*$^{-4}$ and *aha1b*$^{-1}$ mutants carried a 4 bp and 1 bp deletions in *aha1b* gene, respectively (Fig. S4, Supplemental material). All these indel mutations created reading frame shifts that resulted in premature translational termination (Fig. 6). To assess whether these mutations lead to nonsense mediated mRNA decay, we analyzed *aha1a* and *aha1b* mRNA expression by whole mount *in situ* hybridization and real time qRT-PCR. The results showed a clear nonsense mediated mRNA decay in *aha1a*$^{+17/}$, *aha1b*$^{-4}$, and *aha1b*$^{-1}$ mutant embryos (Fig. 7B, F–H), suggesting that they were most likely null mutant alleles. Thus, *aha1a*$^{+17}$and *aha1b*$^{-4}$ mutant alleles were mainly used in the subsequent functional studies.

To test whether loss of *aha1a*, *aha1b*, or both had any effect on muscle development, we analyzed myofiber formation and sarcomere organization in *aha1a*$^{+17}$ and *aha1b*$^{-4}$ single, or double mutant embryos. Zebrafish embryos of WT, *aha1a*$^{+17}$ and *aha1b*$^{-4}$ single, or *aha1a*$^{+17}$; *aha1b*$^{-4}$ double mutants were stained with phalloidin and antibodies against MHC and α-actinin. As shown in Fig. 8A–H, myofibers with clear thick filaments and Z-line organization were observed in slow fibers of both single and double mutant embryos. Moreover, organization of thin filaments and Z-lines also appeared normal in fast myofibers of the single or double mutant embryos (Fig. 8I–P). Together, these data indicate that loss of Aha1a, Aha1b or both had little or no effect on muscle development and myofibril assembly in embryonic skeletal muscles.

Given that *aha1a* and *aha1b* are cochaperones of Hsp90 required for muscle development in *C. elegans* and zebrafish embryos (Du et al., 2008; Frnmkin et al., 2014), we tested whether loss of *aha1a* and *aha1b* could trigger an upregulation of heat shock protein gene expression. *hsp90α1*and *hsp90α2* gene expression was analyzed during myogenesis in *aha1a*$^{+17}$;*aha1b*$^{-4}$ double mutant embryos by whole mount *in situ* hybridization and qRT-PCR and WT. Compared with the WT control (Fig. 9A, C), the results showed that loss of *aha1a* and *aha1b* did not affect the pattern of *hsp90α1* and *hsp90α2* expression in the mutant embryos, respectively (Fig. 9B, D). qRT-PCR analysis confirmed similar levels of *hsp90α1* or *hsp90α2* expression in WT and *aha1a*$^{+17}$;*aha1b*$^{-4}$ mutant embryos (Fig. 9E, F). Collectively, these data indicate that loss of *aha1a* and *aha1b* did not trigger a stress response by upregulation of *hsp90α1* and *hsp90α2* expression in zebrafish embryos.

6. Effects of Aha1 deficiency double mutant on heat shock response

Molecular chaperones and cochaperones play important roles in tress response. Given that *aha1a* and *aha1b* expression was significantly upregulated in fish embryos in response to heat shock, we decided to test whether loss of Aha1a and Aha1b could affect fish embryo survival under heat shock stress. Fish embryos from *aha1a*$^{+17/+}$; *aha1b* $^{-4}$ in-cross and WT control were heat shocked at 48 hpf for 2h at 37℃. Fish survival and overall morphology were analyzed at 50 hpf. No significant difference was detected between heat shock treated WT, heterozygous and homozygous mutant embryos with respect to embryonic survival and morphology (Table 3, Supplemental material). Although pericardial edema was observed in some of the heat shock treated embryos, the edema phenotype was also observed in the WT group and showed no significant correlation between genotype and the edema phenotype (Table 3, Supplemental material).

To test whether muscle development could be affected in the *aha1a*$^{+17}$;*aha1b*$^{-4}$ double mutants by heat shock treatment, we compared myofiber formation in WT and mutant embryos with and without heat shock treatment. Fish embryos of the *aha1a*$^{+17}$; *aha1b*$^{-4}$ double mutants and WT controls were subjected to 37°C heat shock treatment for 1 hr at 20 hpf or 31 hpf. Muscle development was analyzed at 1 hr post heat shock by immunostaining with anti-myosin F59 antibody. No evident difference was detected in myofibers between WT and *aha1a*$^{+17}$;*aha1b*$^{-4}$ mutant embryos (Fig. 10A–D). Both groups showed similar myofiber organization. The lack of significant effect from heat shock on muscle development suggests that stress response might be normal in the absence of Aha1a and Aha1b in the double mutant embryos. To test this idea, we analyzed heat shock protein gene expression in WT and *aha1a*$^{+17}$; *aha1b*$^{-4}$ mutant embryos under a heat shock condition (Fig. 11A–P). Compared with WT control (Fig. 11, B, F, J and N), the data showed a similar upregulation of *hsp40*, *hsp70, hsp90α1*, and *hsp90β* expression in *aha1a*$^{+17}$;*aha1b*$^{-4}$ mutant embryos in response to the heat shock treatment (Fig. 11D, H, L and P). Together, these data indicate that loss of Aha1a and Aha1b had no evident effects on heat shock response in upregulation of heat shock protein gene expression.

7. Loss of Aha1a and Aha1b had no effect on fish survival and muscle growth

A functional proteome is vital to cell and organismal survival. To determine whether loss of Aha1a or Aha1b affects fish viability and growth, we compared fish weights and survival rates among WT, *aha1a*$^{+17}$ and *aha1b*$^{-4}$ single and their double mutants. The mutant fish displayed normal fish growth and rate of survival in adults. The distribution of various genotypes agreed with the Mendelian's law of inheritance (Table 4, Supplemental material). Morphologically, the *aha1a*$^{+17}$and *aha1b*$^{-4}$ single and their double mutants were indistinguishable from the WT siblings (Fig. 12A–C). Similar body weights were found in homozygous and heterozygous mutants compared with WT siblings (Fig. 12D). Together, these data indicate that Aha1a and Aha1b are not essential for zebrafish development, growth, and survival under the normal physiological condition.

To investigate whether there is any phenotype in adult muscle where *aha1a* is strongly expressed, we performed histological analysis on tissue sections of adult trunk muscle. Compared with the WT control (Fig. 13A), no obvious difference was detected in skeletal muscle tissue between WT and the *aha1a*$^{+17}$; *aha1b*$^{-4}$ double mutants (Fig. 13B). Myofibers with similar ranges of diameters were observed in both WT and mutant skeletal muscles. Single fiber analysis revealed comparable average myofiber volume (Fig. 13E), nuclear count (Fig. 13F) and per nuclear volume (Fig. 13G) in multinucleated myofibers of WT and mutant fish. Collectively, these data indicate that Aha1a and Aha1b are not essential for muscle development and growth in zebrafish.

Discussion

In this study, we characterized the expression and function of Aha1a and Aha1b in zebrafish. We demonstrated that *aha1a* and *aha1b* showed distinct patterns of expression in zebrafish embryos and adult tissues. Expression of *aha1a* and *aha1b* was dramatically increased in response to heat shock treatment and *hsp90α1* knockdown. The upregulation of *aha1a*

appeared to be muscle specific. Moreover, Aha1a-GFP fusion protein exhibited a dynamic translocation in muscle cells in response to heat shock. To our surprise, loss of *aha1a* and *aha1b* did not result in any visible phenotype in fish development, growth and survival. Together, our studies indicate although Aha1a and Aha1b are involved in stress response, they are dispensable in zebrafish under normal physiological conditions

Aha1 gene duplication

Gene duplication is the prime driving factor during evolution (Ohno et al., 1968, 1970). Phylogenetic analysis showed that mammals contain two *Aha* paralogous genes, namely *Ahsa1* (Aha1) and *Ahsa2 (Aha2)*. Ahsa2 *(Aha2)* appears to be mammalian specific as *Ahsa2 (Aha2)* orthologs have yet to be identified in non-mammalian species. Two *aha1* homologous genes, *aha1a* and *aha1b* were found in fish species. The two *aha1* genes were likely generated by the extra round of whole genome duplication in teleosts (Espinosa-Cantú et al., 2015; Meyer and Schartl, 1999; Ohno, 1970). It has been shown that duplicated genes from an ancestral gene could perform the same function. It is equally possible that two duplicated genes could diverge during evolution by changing their patterns of expression to fit the need of a certain cell-type-specific function at a given developmental stage (Espinosa-Cantú et al., 2015; Meyer and Schartl, 1999; Ohno, 1970). Data from this study here indicate that Aha1a and Aha1b might have been evolved to have different functions due to their different pattern of expression in trunk muscle and the head region. Aha1a and Aha1b may work in concert with distinct Hsp90 isoforms that are co-expressed with Aha1a or Aha1b. For example, Hsp90α1 specifically expressed in muscle cells, may work with Aha1 to control protein homeostasis in muscle cells. In contrast, Hsp90β and Hsp90αb1 that are strongly expressed in the head region of zebrafish embryos may work with Aha1b to regulate proteostasis in the nerve and other cells of the head region (Comyn and Pilgrim, 2012; Etard et al., 2007; Krone and Sass, 1994).

Aha1 in stress response

Upregulation of heat shock protein gene expression is a common stress response, but how Aha1 react to stress in vertebrate systems is largely unknown. Previous studies have demonstrated that heat shock of zebrafish embryos induced a large array of HSP gene expression including Hsp40, Hsp70s and Hsp90s (Cai et al., 2019; Krone et al., 1997, 2003, 2007). We showed in this study that *aha1a* and *aha1b* expression was dramatically upregulated by acute heat shock treatment of zebrafish embryos. The upregulation of *aha1a* and *aha1b* expression in response to heat shock is consistent with their potential roles as a Hsp90 cochaperones to participate in stress response. Interestingly, *aha1a* and *aha1b* exhibited distinct patterns of upregulation of expression in response to heat shock. *aha1a* was predominantly upregulated in trunk muscles of fish embryos whereas *aha1b* expression was broadly upregulated with a stronger expression in the head region, especially at 2 dpf. The distinct patterns of *aha1a* and *aha1b* upregulation were largely complementary and also in agreement with their normal pattern of expression in the trunk muscle and the head region, respectively. Additionally, we showed that knockdown of *hsp90a1* but not *hsp90α2* resulted in increased *aha1a* and *aha1b* expression at 24 hpf. Interestingly, the increased expression was mainly restricted to trunk muscle of *hsp90α1* knockdown embryo. This is consistent with previous reports that Hsp90α1 but not Hsp90α2 plays a critical role in

myosin protein folding and sarcomere assembly in zebrafish skeletal muscles (Du et al., 2008; Etard et al., 2007; Hawkins et al., 2008). Considering that *aha1a* is normally expressed in developing muscles of the zebrafish embryos, these data indicated that Aha1a might be involved in Hsp90α1 function in muscle cell differentiation under both normal and stress conditions, while Aha1b might be only involved under stress conditions in muscle cells.

In addition to the distinct pattern of gene expression in stress response, Aha1a and Ah1b differed in their protein subcellular localization in response to heat shock induced stress. Aha1a-GFP protein showed a dynamic translocation from the Z-line to the myosin enriched A-bands when fish embryos were stressed by heat shock, while no dynamic translocation was detected with Aha1b-GFP in response to heat shock. The Aha1a-GFP translocation is very similar to previous findings with Hsp90α1 in zebrafish (Etard et al., 2008). Etard and colleagues demonstrated that in response to stress or damage to the myofiber, myosin chaperones, Unc45b and Hsp90a, dissociate from the Z line and transiently associate with myosin, suggesting that the Z lines may serve as a reservoir for chaperone proteins from which they can be mobilized in a reversible manner by damage to the myofibrils. Excitingly, the chaperone translocation has been observed in skeletal myopathy. Unger and colleagues showed that translocation of molecular chaperones to the titin springs is common in skeletal myopathy patients and affects sarcomere function (Unger et al., 2017). Data from the protein translocation and upregulation of expression further support idea that Aha1a is likely involved in Hsp90α1 function in muscle protein folding and sarcomere assembly in response to stress.

Requirement of Aha1 in organismal survival

Large bodies of evidence indicate that Aha1 is essential for yeast survival under stress conditions. Panaretou and colleagues demonstrated that although yeast mutant with Aha1 deletion grew normally under normal physiological temperatures, the Aha1 mutant showed compromised Hsp90 function and survival in elevated temperatures (Panaretou et al., 2002). Similar findings were reported for Hch1, a shorter homolog pf Aha1 in yeast (Panaretou et al., 2002; Armstrong et al., 2012). As expected, deletion of and Aha1 and Hch1 together further compromised yeast survival at higher temperatures (Panaretou et al., 2002), especially under non-optimal growth conditions when Hsp90 levels were limited (Lotz et al., 2003). Biochemical analysis showed that Aha1 and Hch1 were essential cochaperones of Hsp90 and played a vital role in Hsp90 cycle and client protein activation (Lotz et al., 2003; Panaretou et al., 2002). Genetic analysis in *C. elegans* revealed similar findings with respect to Aha1 function in muscle development and animal mobility (Frumkin et al., 2014). Frumkin and colleagues reported that knockdown of Aha1 (ahsa-1) expression in *Caenorhabditis elegans* had no apparent phenotype under normal condition. However, under stress conditions from *unc*-45 temperature-sensitive mutation and Hsp90 deficiency, Aha1 was found to be critical for muscle homeostasis and integrity (Frumkin et al., 2014).

We showed in this study that loss of Aha1a, Aha1b or both had no effect on zebrafish embryonic development, growth and survival. The lack of a clear phenotype under normal physiological condition is consistent with previous findings with *aha1* mutants in yeast and *C. elegans* (Frumkin et al., 2014; Lotz et al., 2003; Panaretou et al., 2002). However, to our

surprise, muscle development and fish survival also appeared normal in Aaha1a and Aha1b double mutant subjected to acute heat shock stress. Currently, it is not clear why zebrafish mutants showed no visible abnormality under stressed conditions. One possibility is that the stress conditions used in this study were transient and not sufficient to cause visible defects in the *aha1* mutants. Secondly, it is generally believed that Aha1 acts as an activator of Hsp90 ATPase that stimulates Hsp90 function in the proteostasis network. Although ATPase activity is clearly necessary for efficient function of Hsp90 (Obermann et al., 1998; Panaretou et al., 1998), the absolute requirement for ATP hydrolysis has been questioned in a recent study (Zierer et al., 2016). Zierer and colleagues showed that some yeast mutants with lower or undetectable Hsp90 ATPase activity were viable. Thirdly, it has been reported that Hsp90 functions in nascent polypeptides folding process downstream from hsp70 is independent of co-chaperone (Moran Luengo et al, 2019; Sun et al, 2012). The lack of muscle phenotype in Aha1a and Aha1b knockout mutant embryos is consistent with the idea that Hsp90α1 could function normally in myosin folding and sarcomere assembly under normal physiological conditions. Loss of Aha1 activity might only cause minor effects and our limited phenotypical characterization might not reveal these minor impacts on fish development, growth, and physiology. Lastly, we cannot rule out the possibility that other factors may play a redundant role in the stress response in the absence of Aha1. Consistent with this idea, we showed that loss of *aha1a* and *aha1b* did not affect the stress response in the mutant fish embryos from heat shock. A clear upregulation of Hsp40, Hsp70 and Hsp90 gene expression was observed in the heat shock treated *aha1a*; *aha1b* mutant embryos. These upregulated heat shock proteins might compensate for the lack of Aha1 to maintain proteostasis under the stress condition.

Aha1 animal model in neurodegenerative and other diseases

Progressive accumulation of misfolded proteins is a common feature in neurodegenerative disorders and aging. Protein aggregation and inclusion bodies formation have been reported in the progression of Parkinson's disease (PD), Alzheimer's disease (AD), Huntington's disease (HD), Prion disease, amyotrophic lateral sclerosis (ALS) and spinal and bulbar muscular atrophy (SBMA) (Ross and Poirier, 2004; Soto and Pritzkow, 2018; Sweeney et al., 2017; Lashuel, 2021, Kumar et al., 2016). Many of the disease-causing proteins, such as Tau, huntingtin (Htt), and polyglutamine androgen receptor are client proteins of Hsp90/Aha1/Hsp70 chaperone machinery. It is generally believed that HSP chaperones and cochaperones are important components of the proteostasis network that assists protein folding, prevents aggregation, and promotes refolding of denatured model substrates. However, recent studies demonstrated that under pathological conditions, Hsp90 and Aha1 can promote the accumulation of misfolded pathogenic Tau protein and drive the production of pathological Tau aggregates in Tau transgenic mouse model and aged wild-type mice (Criado-Marrero et al., 2021; Shelton et al., 2017). Histological analysis in postmortem AD brain revealed that Aha1 colocalized with pathogenic Tau (Shelton et al., 2017). Treatment with Aha1 inhibitors that block its interaction with Hsp90 could help reduce Tau fibril aggregation. These studies raise the question of potential negative impact of Hsp90/Aha1 activity on neurodegenerative diseases.

The negative impact of Hsp90/Aha1 function has been observed in diseases progression of other genetic diseases involved in protein quality control. Wang and colleagues showed that downregulation of Aha1 could rescue misfolding of CFTR in cystic fibrosis (Wang et al., 2006), reduce tau accumulation in cultured cells (Shelton et al., 2017). A study in zebrafish demonstrated that Ahsa1 and Hsp90 activity confers more severe craniofacial phenotypes in a zebrafish model of hypoparathyroidism, sensorineural deafness and renal dysplasia (HDR) (Sheehan-Rooney et al., 2013). Overexpression Ahsa1 in promoted severe craniofacial phenotypes in zebrafish model of HDR syndrome, while knockdown of Aha1a could alleviate the severity of the craniofacial phenotypes (Sheehan-Rooney et al., 2013). All these studies were performed with mammalian cells in culture or knockdown animal models. Our *aha1a* and *aha1b* zebrafish mutants represent the first vertebrate model with total loss of Aha1 activity. The *aha1a* and *aha1b* mutant zebrafish thus provide useful models to study their role neurodegenerative and other genetic diseases from dysfunction of the proteostasis network.

Supplementary Material

Refer to Web version on PubMed Central for supplementary material.

Acknowledgments

We thank Mr. Chenyu Zhang for assistance in bioinformatic analysis. This research was supported by grant funding from the National Institute of Health (R01AR072703 to SD). HX, HW and JZ were supported by student fellowship and visiting scholarship from Chinese Scholarship Council.

Nonstandard Abbreviations:

hpf	hours-post-fertilization
dpf	days-post-fertilization

References:

Armstrong H, Wolmarans A, Mercier R, Mai B & LaPointe P, 2012. The co-chaperone Hch1 regulates Hsp90 function differently than its homologue Aha1 and confers sensitivity to yeast to the Hsp90 inhibitor NVP-AUY922.PLoS One 7, e49322, doi: 10.1371/journal.pone.0049322. [PubMed: 23166640]

Benjamin IJ, & McMillan DR,1998. Stress (heat shock) proteins: molecular chaperones in cardiovascular biology and disease. Circulation research, 83(2), 117–132. 10.1161/01.res.83.2.117 [PubMed: 9686751]

Biebl MM, Buchner J, 2019. Structure, function, and regulation of the Hsp90 machinery. Cold Spring Harb. Perspect. Biol, 11, p. a034017. [PubMed: 30745292]

Biebl MM, Riedl M, & Buchner J,2020. Hsp90 Co-chaperones Form Plastic Genetic Networks Adapted to Client Maturation. Cell reports, 32(8), 108063. 10.1016/j.celrep.2020.108063 [PubMed: 32846121]

Bhattacharya K, Weidenauer L, Luengo TM et al. ,2020. The Hsp70-Hsp90 co-chaperone Hop/Stip1 shifts the proteostatic balance from folding towards degradation. Nat Commun 11, 5975. 10.1038/s41467-020-19783-w [PubMed: 33239621]

Borkovich KA, Farrelly FW, Finkelstein DB, Tauhen J and Lindquist S ,1989. hsp82 is an essential protein that is required in higher concentrations for growth of cells at higher temperatures. Mol. Cell. Biol 9, 3919–3930. [PubMed: 2674684]

Buchberger A, Bukau B, & Sommer T,2010. Protein quality control in the cytosol and the endoplasmic reticulum: brothers in arms. Molecular cell, 40(2), 238–252. 10.1016/j.molcel.2010.10.001 [PubMed: 20965419]

Cáceres RA, Chavez T, Maestro D, Palanca AR, Bolado P, Madrazo F, Aires A, Cortajarena AL, Villar AV., 2018. Reduction of cardiac TGFβ-mediated profibrotic events by inhibition of Hsp90 with engineered protein. J Mol Cell Cardiol.123:75–87. doi: 10.1016/j.yjmcc.2018.08.016. [PubMed: 30193958]

Cai M, Si Y, Zhang J, Tian Z, & Du S,2018. Zebrafish Embryonic Slow Muscle Is a Rapid System for Genetic Analysis of Sarcomere Organization by CRISPR/Cas9, but Not NgAgo. Marine biotechnology (New York, N.Y.), 20(2), 168–181. 10.1007/s10126-018-9794-8 [PubMed: 29374849]

Cai M, Han L, Liu L, He F, Chu W, Zhang J, Tian Z, & Du S, 2019. Defective sarcomere assembly in smyd1a and smyd1b zebrafish mutants. FASEB journal. 33(5), 6209–6225. 10.1096/fj.201801578R [PubMed: 30817176]

Cermak T 1, Doyle EL, Christian M, Wang L, Zhang Y, Schmidt C, Baller JA, Somia NV, Bogdanove AJ, Voytas DF, 2011. Efficient design and assembly of custom TALEN and other TAL effector-based constructs for DNA targeting. Nucleic Acids Res. 39(12):e82. [PubMed: 21493687]

Chen S, Smith DF., 1998. Hop as an adaptor in the heat shock protein 70 (Hsp70) and hsp90 chaperone machinery. J Biol Chem. 25;273(52):35194–200. doi: 10.1074/jbc.273.52.35194. [PubMed: 9857057]

Chen B, Zhong D, & Monteiro A, 2006. Comparative genomics and evolution of the HSP90 family of genes across all kingdoms of organisms. BMC genomics, 7, 156. 10.1186/1471-2164-7-156 [PubMed: 16780600]

Clark KJ, Balciunas D, Pogoda HM, Ding Y, Westcot SE, Bedell VM, Greenwood TM, Urban MD, Skuster KJ, Petzold AM, Ni J, Nielsen AL, Patowary A, Scaria V, Sivasubbu S, Xu X, Hammerschmidt M, Ekker SC,2011. In vivo protein trapping produces a functional expression codex of the vertebrate proteome. Nat Methods. 8(6), 506–515. [PubMed: 21552255]

Comyn SA, Pilgrim D., 2012. Lack of developmental redundancy between Unc45 proteins in zebrafish muscle development. PLoS One 7:e48861 [PubMed: 23144999]

Criado-Marrero M, Gebru NT, Blazier DM, Gould LA, Baker JD, Beaulieu-Abdelahad D, Blair LJ, 2021. Hsp90 co-chaperones, FKBP52 and Aha1, promote tau pathogenesis in aged wild-type mice. Acta Neuropathol. Commun 9, 65. [PubMed: 33832539]

Cutforth T, Rubin GM, 1994. Mutations in Hsp83 and cdc37 impair signaling by the sevenless receptor tyrosine kinase in Drosophila. Cell. 77: 1027–1036. [PubMed: 8020093]

Du SJ, Li H, Bian Y, Zhong Y, 2008. Heat-shock protein 90alpha1 is required for organized myofibril assembly in skeletal muscles of zebrafish embryos. Proc Natl Acad Sci U S A 105(2):554. [PubMed: 18182494]

Espinosa-Cantú A, Ascencio D, Barona-Gómez F, DeLuna A, 2015. Gene duplication and the evolution of moonlighting proteins. Front Genet. 6, 227. [PubMed: 26217376]

Etard C, Behra M, Fischer N, Hutcheson D, Geisler R, Strähle U, 2007. The UCS factor Steif/Unc-45b interacts with the heat shock protein Hsp90a during myofibrillogenesis. Dev Biol. 308(1):133–43. [PubMed: 17586488]

Etard C, Armant O, Roostalu U, Gourain V, Ferg M, Strähle U, 2015. Loss of function of myosin chaperones triggers Hsf1-mediated transcriptional response in skeletal muscle cells. Genome Biol. 16:267. doi: 10.1186/s13059-015-0825-8. [PubMed: 26631063]

Etard C, Roostalu U, & Strähle U,2008. Shuttling of the chaperones Unc45b and Hsp90a between the A band and the Z line of the myofibril. J Cell Biol. 180(6), 1163–1175. 10.1083/jcb.200709128 [PubMed: 18347070]

Frumkin A, Dror S, Pokrzywa W, Bar-Lavan Y, Karady I, Hoppe T, & Ben-Zvi A ,2014. Challenging muscle homeostasis uncovers novel chaperone interactions in Caenorhabditis elegans. Frontiers in molecular biosciences, 1, 21. 10.3389/fmolb.2014.00021 [PubMed: 25988162]

Gaiser AM, Kaiser CJ, Haslbeck V, and Richter K, 2011. Downregulation of the Hsp90 system causes defects in muscle cells of Caenorhabditis elegans. PLoS ONE 6:e25485. doi: 10.1371/journal.pone.0025485 [PubMed: 21980476]

Ganassi M, Badodi S, Ortuste Quiroga HP et al. , 2018. Myogenin promotes myocyte fusion to balance fibre number and size. Nat Commun 9, 4232. 10.1038/s41467-018-06583-6 [PubMed: 30315160]

Ganassi M, Zammit PS, & Hughes SM, 2021. Isolation of Myofibres and Culture of Muscle Stem Cells from Adult Zebrafish. Bio-protocol, 11(17), e4149. 10.21769/BioProtoc.4149 [PubMed: 34604454]

García R, Merino D, Gómez JM, Nistal JF, Hurlé MA, Cortajarena AL, Villar AV., 2016. Extracellular heat shock protein 90 binding to TGFβ receptor I participates in TGFβ-mediated collagen production in myocardial fibroblasts. Cell Signal. 28(10):1563–79. doi: 10.1016/j.cellsig.2016.07.003. [PubMed: 27418101]

Geller R, Pechmann S, Acevedo A, Andino R, & Frydman J, 2018. Hsp90 shapes protein and RNA evolution to balance trade-offs between protein stability and aggregation. Nature communications, 9(1), 1781. 10.1038/s41467-018-04203-x

Grad I, Cederroth CR, Walicki J, Grey C, Barluenga S, Winssinger N, De Massy B, Nef S, and Picard D, 2010. The molecular chaperone Hsp90α is required for meiotic progression of spermatocytes beyond pachytene in the mouse. PLoS One 5:e15770. [PubMed: 21209834]

Hawkins TA, Haramis AP, Etard C, Prodromou C, Vaughan CK, Ashworth R, Ray S, Behra M, Holder N, Talbot WS, Pearl LH, Strähle U, Wilson SW, 2008. The ATPase-dependent chaperoning activity of Hsp90a regulates thick filament formation and integration during skeletal muscle myofibrillogenesis. Development 135(6):1147–56. doi: 10.1242/dev.018150. [PubMed: 18256191]

Hawle P, et al. , 2008. The middle domain of Hsp90 acts as a discriminator between different types of client proteins. Mol Cell Biol. 26:8385–8395.

Hendrick JP, & Hartl FU, 1993. Molecular chaperone functions of heat-shock proteins. Annual review of biochemistry, 62, 349–384. 10.1146/annurev.bi.62.070193.002025

Horvat NK et al. , 2014. A mutation in the catalytic loop of hsp90 specifically impairs ATPase stimulation by aha1p, but not hch1p. J Mol Biol 426, 2379–2392, doi: 10.1016/j.jmb. [PubMed: 24726918]

Hoter A, El-Sabban ME, & Naim HY,2018. The HSP90 Family: Structure, Regulation, Function, and Implications in Health and Disease. International journal of molecular sciences, 19(9), 2560. 10.3390/ijms19092560 [PubMed: 30158430]

Hwang WY, Fu Y, Reyon D, Maeder ML, Tsai SQ, Sander JD, Peterson RT, Yeh JR, Joung JK. Efficient genome editing in zebrafish using a CRISPR-Cas system. Nat Biotechnol. 2013 Mar;31(3):227–9. doi: 10.1038/nbt.2501. Epub 2013 Jan 29. [PubMed: 23360964]

Ichiyanagi T, Imai T, Kajiwara C, Mizukami S, Nakai A, Nakayama T, & Udono H,2010. Essential role of endogenous heat shock protein 90 of dendritic cells in antigen cross-presentation. Journal of immunology (Baltimore, Md. : 1950), 185(5), 2693–2700. 10.4049/jimmunol.1000821 [PubMed: 20668218]

Imai T, Kato Y, Kajiwara C, Mizukami S, Ishige I, Ichiyanagi T, Hikida M, Wang JY, & Udono H,2011. Heat shock protein 90 (HSP90) contributes to cytosolic translocation of extracellular antigen for cross-presentation by dendritic cells. Proceedings of the National Academy of Sciences of the United States of America, 108(39), 16363–16368. 10.1073/pnas.1108372108 [PubMed: 21930907]

Jiao S, Xu R, Du S. Smyd1 is essential for myosin expression and sarcomere organization in craniofacial, extraocular, and cardiac muscles., 2021. J Genet Genomics. 2021 Mar 20;48(3):208–218. doi: 10.1016/j.jgg.2021.03.004. [PubMed: 33958316]

Johnson AD, & Krieg PA (1995). A Xenopus laevis gene encoding EF-1 alpha S, the somatic form of elongation factor 1 alpha: sequence, structure, and identification of regulatory elements required for embryonic transcription. Developmental genetics, 17(3), 280–290. [PubMed: 8565334]

Kajiwara C, Kondo S, Uda S, 2012. Spermatogenesis arrest caused by conditional deletion of Hsp90α in adult mice. Biol Open. 1(10):977–982. doi:10.1242/bio.2012646. [PubMed: 23213375]

Kumar R, Kumari B, and Kumar M,2016. PredHSP: sequence based proteome-wide heat shock protein prediction and classification tool to unlock the stress biology. PLoS ONE 11:e0155872. doi: 10.1371/journal.pone.0155872 [PubMed: 27195495]

Krone PH, Evans TG, Blechinger SR., 2003. Heat shock gene expression and function during zebrafish embryogenesis. Semin Cell Dev Biol. 14:267–274.1084–9521. [PubMed: 14986856]

Krone PH, Lele Z, Sass JB, 2007. Heat shock genes and the heat shock response in zebrafish embryos. Biochem Cell Biol 75(5):487–97.

Krone PH, Sass JB, 1994. HSP 90 alpha and HSP 90 beta genes are present in the zebrafish and are differentially regulated in developing embryos. Biochem Biophys Res Commun 204(2):746–52. doi: 10.1006/bbrc.1994.2522. [PubMed: 7980538]

Krone PH, Sass JB, Lele Z., 1997. Heat shock protein gene expression during embryonic development of the zebrafish. Cell Mol Life Sci. 53(1):122–9. doi: 10.1007/pl00000574. [PubMed: 9117992]

Lackie RE, Maciejewski A, Ostapchenko VG, Marques-Lopes J, Choy WY, Duennwald ML, Prado VF, & Prado M,2017. The Hsp70/Hsp90 Chaperone Machinery in Neurodegenerative Diseases. Frontiers in neuroscience, 11, 254. 10.3389/fnins.2017.00254 [PubMed: 28559789]

Lashuel Hilal A.,2021. Rethinking protein aggregation and drug discovery in neurodegenerative diseases: Why we need to embrace complexity?. Current opinion in chemical biology vol. 64: 67–75. doi:10.1016/j.cbpa.2021.05.006 [PubMed: 34174698]

Li H, Zhong Y, Wang Z, Gao J, Xu J, Chu W, Zhang J, Fang S, & Du SJ, 2013. Smyd1b is required for skeletal and cardiac muscle function in zebrafish. Molecular biology of the cell, 24(22), 3511–3521. 10.1091/mbc.E13-06-0352 [PubMed: 24068325]

Li J, Richter K & Buchner J,2011. Mixed Hsp90–cochaperone complexes are important for the progression of the reaction cycle. Nat Struct Mol Biol 18, 61–66. 10.1038/nsmb.1965 [PubMed: 21170051]

Li J, Soroka J, & Buchner J,2012. The Hsp90 chaperone machinery: conformational dynamics and regulation by co-chaperones. Biochimica et biophysica acta, 1823(3), 624–635. 10.1016/j.bbamcr.2011.09.003 [PubMed: 21951723]

Li J, & Buchner J,2013. Structure, function and regulation of the hsp90 machinery. Biomedical journal, 36(3), 106–117. 10.4103/2319-4170.113230 [PubMed: 23806880]

Lotz GP, Lin H, Harst A, Obermann WM, 2003. Aha1 binds to the middle domain of Hsp90, contributes to client protein activation, and stimulates the ATPase activity of the molecular chaperone. J Biol Chem 278(19):17228–35. [PubMed: 12604615]

Meyer A, Schartl M, 1999. Gene and genome duplications in vertebrates: the one-to-four (-to-eight in fish) rule and the evolution of novel gene functions. Current Opinion in Cell Biology 11, 699–704. [PubMed: 10600714]

Meyer P et al. , 2004. Structural basis for recruitment of the ATPase activator Aha1 to the Hsp90 chaperone machinery. Embo J 23, 1402–1410. [PubMed: 15039704]

Moran Luengo T, Mayer MP, Rudiger SGD., 2019. The Hsp70-Hsp90 chaperone cascade in protein folding. Trends Cell Biol 29: 164–177. [PubMed: 30502916]

Nasevicius A, Ekker SC Effective targeted gene “knockdown” in zebrafish. Nat Genet. 2000, 26:216–20. [PubMed: 11017081]

Ohno et al. , Ohno S, Wolf U, Atkin NB, 1968. Evolution from fish to mammals by gene duplication. Hereditas pp. 169–187. [PubMed: 5662632]

Ohno S Ohno, 1970. Evolution by Gene Duplication. London: George Alien & Unwin Ltd, Berlin. Springer-Verlag.

Obermann WM, Sondermann H, Russo AA, Pavletich NP, & Hartl FU,1998. In vivo function of Hsp90 is dependent on ATP binding and ATP hydrolysis. The Journal of cell biology, 143(4), 901–910. 10.1083/jcb.143.4.901 [PubMed: 9817749]

Pratt WB, & Toft DO,2003. Regulation of signaling protein function and trafficking by the hsp90/hsp70-based chaperone machinery. Experimental biology and medicine (Maywood, N.J.), 228(2), 111–133. 10.1177/153537020322800201.

Panaretou B et al. ,1998. ATP binding and hydrolysis are essential to the function of the Hsp90 molecular chaperone in vivo. Embo J 17, 4829–4836, doi: 10.1093/emboj/17.16.4829. [PubMed: 9707442]

Panaretou B, Siligardi G, Meyer P, Maloney A, Sullivan JK, Singh S, Millson SH, Clarke PA, Naaby-Hansen S, Stein R, Cramer R, Mollapour M, Workman P, Piper PW, Pearl LH and Prodromou C, 2002. Activation of the ATPase activity of hsp90 by the stress-regulated cochaperone aha1. Mol Cell 10, 1307–1318. [PubMed: 12504007]

Picard D, Khursheed B, Garabedian M et al. , 1990. Reduced levels of hsp90 compromise steroid receptor action in vivo. Nature 348, 166–168. 10.1038/348166a0 [PubMed: 2234079]

Prodromou C, Panaretou B, Chohan S, Siligardi G, O'Brien R, Ladbury JE, Roe SM, Piper PW, & Pearl LH,2000. The ATPase cycle of Hsp90 drives a molecular 'clamp' via transient dimerization of the N-terminal domains. The EMBO journal, 19(16), 4383–4392. 10.1093/emboj/19.16.438 [PubMed: 10944121]

Retzlaff M, Hagn F, Mitschke L, Hessling M, Gugel F, Kessler H, Richter K, Buchner J., 2010. Asymmetric activation of the hsp90 dimer by its cochaperone aha1. Mol Cell. 12;37(3):344–54. doi: 10.1016/j.molcel.2010.01.006. [PubMed: 20159554]

Roe SM, Ali MM, Meyer P, Vaughan CK, Panaretou B, Piper PW, Prodromou C, Pearl LH., 2004. The Mechanism of Hsp90 regulation by the protein kinase-specific cochaperone p50(cdc37). Cell. Jan 9;116(1):87–98. doi: 10.1016/s0092-8674(03)01027-4. [PubMed: 14718169]

Ross CA, & Poirier MA,2004. Protein aggregation and neurodegenerative disease. Nature medicine, 10 Suppl, S10–S17. 10.1038/nm1066

Roy S, Wolff C, Ingham PW., 2001. The u-boot mutation identifies a Hedgehog-regulated myogenic switch for fiber-type diversification in the zebrafish embryo. Genes Dev.15;15(12):1563–76. doi: 10.1101/gad.195801. [PubMed: 11410536]

Rutherford S, Lindquist S, 1998. Hsp90 as a capacitor for morphological evolution. Nature 396, 336–342. 10.1038/24550 [PubMed: 9845070]

Sahasrabudhe P, Rohrberg J, Biebl MM, Rutz DA & Buchner J, 2017. The plasticity of the Hsp90 Co-chaperone system. Mol. Cell 67, 947–961 e5. [PubMed: 28890336]

Schopf F, Biebl M & Buchner J, 2017. The HSP90 chaperone machinery. Nat Rev Mol Cell Biol 18, 345–36. [PubMed: 28429788]

Sheehan-Rooney K, Swartz ME, Zhao F, Liu D, & Eberhart JK, 2013. Ahsa1 and Hsp90 activity confers more severe craniofacial phenotypes in a zebrafish model of hypoparathyroidism, sensorineural deafness and renal dysplasia (HDR). Disease models & mechanisms, 6(5), 1285–1291. 10.1242/dmm.011965 [PubMed: 23720234]

Shelton LB, Baker JD, Zheng D, et al. , 2017. Hsp90 activator Aha1 drives production of pathological tau aggregates. Proc Natl Acad Sci U S A. 114(36):9707–9712. doi:10.1073/pnas.1707039114. [PubMed: 28827321]

Shi J, Cai M, Si Y, Zhang J, Du S., 2018. Knockout of myomaker results in defective myoblast fusion, reduced muscle growth and increased adipocyte infiltration in zebrafish skeletal muscle. Hum Mol Genet. 15;27(20):3542–3554. doi: 10.1093/hmg/ddy268. [PubMed: 30016436]

Somogyvári M, Gecse E & Sőti C, 2018. DAF-21/Hsp90 is required for C. elegans longevity by ensuring DAF-16/FOXO isoform A function. Sci Rep 8, 12048. 10.1038/s41598-018-30592-6 [PubMed: 30104664]

Soto C, Pritzkow S,2018. Protein misfolding, aggregation, and conformational strains in neurodegenerative diseases. Nat Neurosci 21, 1332–1340. 10.1038/s41593-018-0235-9 [PubMed: 30250260]

Sreedhar AS, Kalmár E, Csermely P, and Shen YF, 2004. Hsp90 isoforms: functions, expression and clinical importance. FEBS Lett 562:11–15. [PubMed: 15069952]

Sun L, Prince T, Manjarrez JR, Scroggins BT, Matts RL., 2012. Characterization of the interaction of Aha1 with components of the Hsp90 chaperone machine and client proteins. Biochim Biophys Acta. Jun;1823(6):1092–101. doi: 10.1016/j.bbamcr.2012.03.014. [PubMed: 22504172]

Sweeney P, Park H, Baumann M et al. ,2017. Protein misfolding in neurodegenerative diseases: implications and strategies. Transl Neurodegener 6, 6. 10.1186/s40035-017-0077-5 [PubMed: 28293421]

Tan XG, Rotllant J, Li H, DeDeyne P and Du SJ, 2006. SmyD1, a histone methyltransferase, is required for myofibril organization and muscle contraction in zebrafish embryos. Proc. Natl. Academy. Sci. USA 103, 2713–2718.

Thisse C, Thisse B, 2008. High-resolution in situ hybridization to whole-mount zebrafish embryos. Nat Protoc 3, 59–69. 10.1038/nprot.2007.514 [PubMed: 18193022]

Taipale M, Jarosz DF, & Lindquist S (2010). HSP90 at the hub of protein homeostasis: emerging mechanistic insights. Nature reviews. Molecular cell biology, 11(7), 515–528. 10.1038/nrm2918 [PubMed: 20531426]

Unger A, Beckendorf L, Böhme P, Kley R, von Frieling-Salewsky M, Lochmüller H, Schröder R, Fürst DO, Vorgerd M, & Linke WA,2017. Translocation of molecular chaperones to the titin springs is common in skeletal myopathy patients and affects sarcomere function. Acta neuropathologica communications, 5(1), 72. 10.1186/s40478-017-0474-0 [PubMed: 28915917]

Urasaki A, Morvan G, & Kawakami K,2006. Functional dissection of the Tol2 transposable element identified the minimal cis-sequence and a highly repetitive sequence in the subterminal region essential for transposition. Genetics, 174(2), 639–649. 10.1534/genetics.106.060244 [PubMed: 16959904]

Vabulas RM, Raychaudhuri S, Hayer-Hartl M, & Hartl FU,2010. Protein folding in the cytoplasm and the heat shock response. Cold Spring Harbor perspectives in biology, 2(12), a004390. 10.1101/cshperspect.a004390 [PubMed: 21123396]

van der Straten A, Rommel C, Dickson B, Hafen E., 1997. The heat shock protein 83 (Hsp83) is required for Raf-mediated signalling in Drosophila. EMBO J. 16: 1961–1969. [PubMed: 9155022]

Voss AK, Thomas T, and Gruss P, 2000. Mice lacking HSP90beta fail to develop a placental labyrinth. Development 127, 1–11. [PubMed: 10654595]

Wang W, Vinocur B, Shoseyov O, & Altman A,2004. Role of plant heat-shock proteins and molecular chaperones in the abiotic stress response. Trends in plant science, 9(5), 244–252. 10.1016/j.tplants.2004.03.006 [PubMed: 15130550]

Wang X et al. , 2006. Hsp90 cochaperone Aha1 downregulation rescues misfolding of CFTR in cystic fibrosis. Cell 127, 803–815. [PubMed: 17110338]

Wolmarans A, Lee B, Spyracopoulos L et al. , 2016. The Mechanism of Hsp90 ATPase Stimulation by Aha1. Sci Rep 6, 33179 . 10.1038/srep33179 [PubMed: 27615124]

Wu Y, Zheng X, Ding Y, Zhou M, Wei Z, Liu T, & Liao K,2020. The molecular chaperone Hsp90α deficiency causes retinal degeneration by disrupting Golgi organization and vesicle transportation in photoreceptors. Journal of molecular cell biology, 12(3), 216–229. [PubMed: 31408169]

Xu J, Gao J, Li JL, Xue LY, Clark KJ, Ekker SC, Du SJ,2012. Functional Analysis of Slow Myosin Heavy Chain 1 and Myomesin-3 in Sarcomere Organization in Zebrafish Embryonic Slow Muscles. J Genet Genomics. 39, 69–80. [PubMed: 22361506]

Yue L, Karr TL, Nathan DF, Swift H, Srinivasan S et al. , 1999. Genetic analysis of viable Hsp90 alleles reveals a critical role in Drosophila spermatogenesis. Genetics 151: 1065–1079. [PubMed: 10049923]

Zierer BK, Rübbelke M, Tippel F, Madl T, Schopf FH, Rutz DA, et al. , 2016. Importance of cycle timing for the function of the molecular chaperone Hsp90. Nat. Struct. Mol. Biol 23, 1020–1028. [PubMed: 27723736]

Zuehlke A, Johnson JL., 2010. Hsp90 and co-chaperones twist the functions of diverse client proteins. Biopolymers. Mar;93(3):211–7. doi: 10.1002/bip.21292.

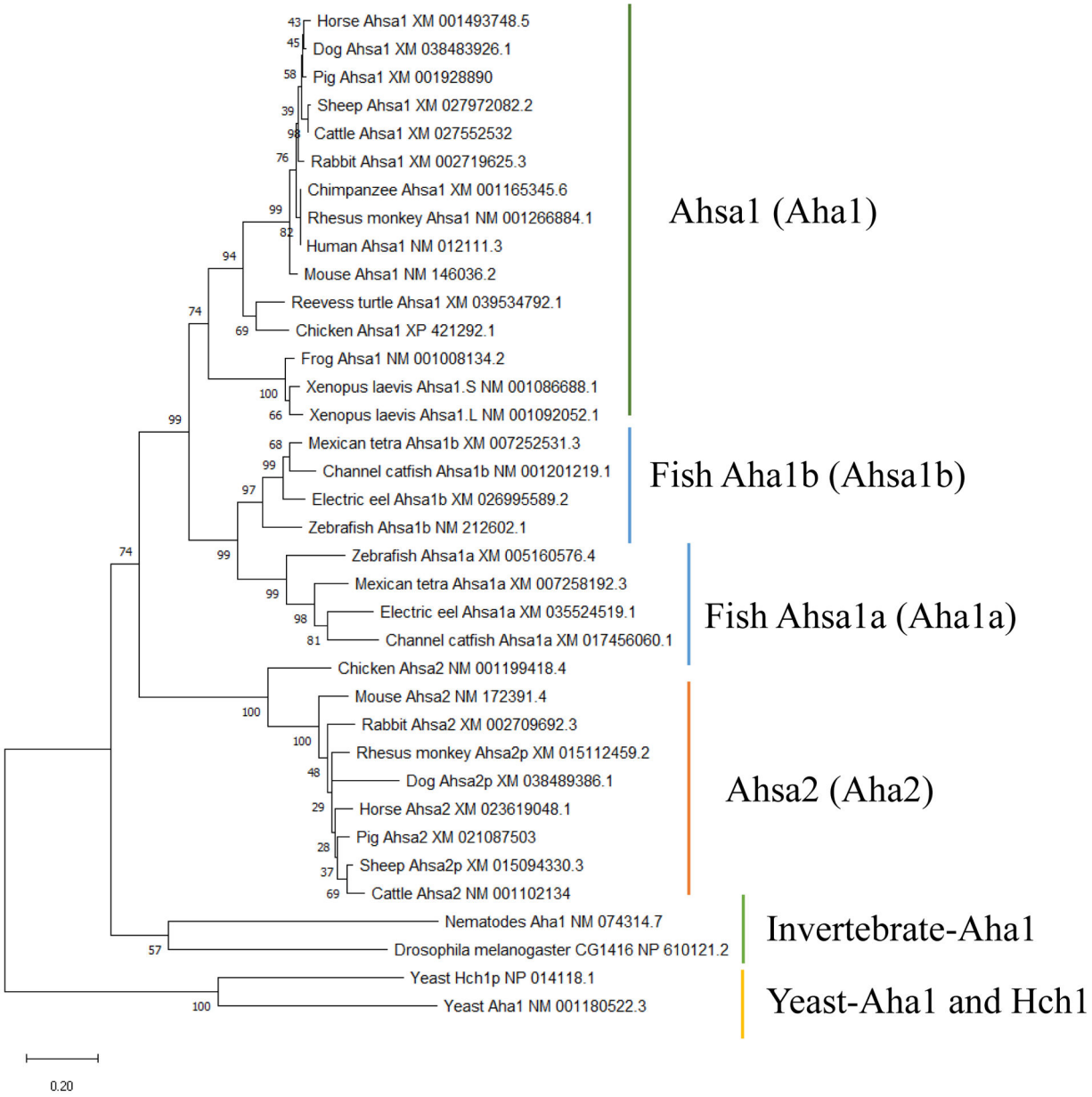

Figure 1. Phylogenetic analysis of Aha-type co-chaperones among different species.

Phylogenetic tree was developed based on Aha-type protein sequences from yeast to mammals. The Aha-type cochaperones could be divided into four branches. The first branch is made up of the Ahsa1 (Aha1), Fish Aha1a and Aha1b subgroups. The other three branches are Ahsa2 (Aha2), invertebrate Aha1 and yeast Aha1 and Hch1, respectively.

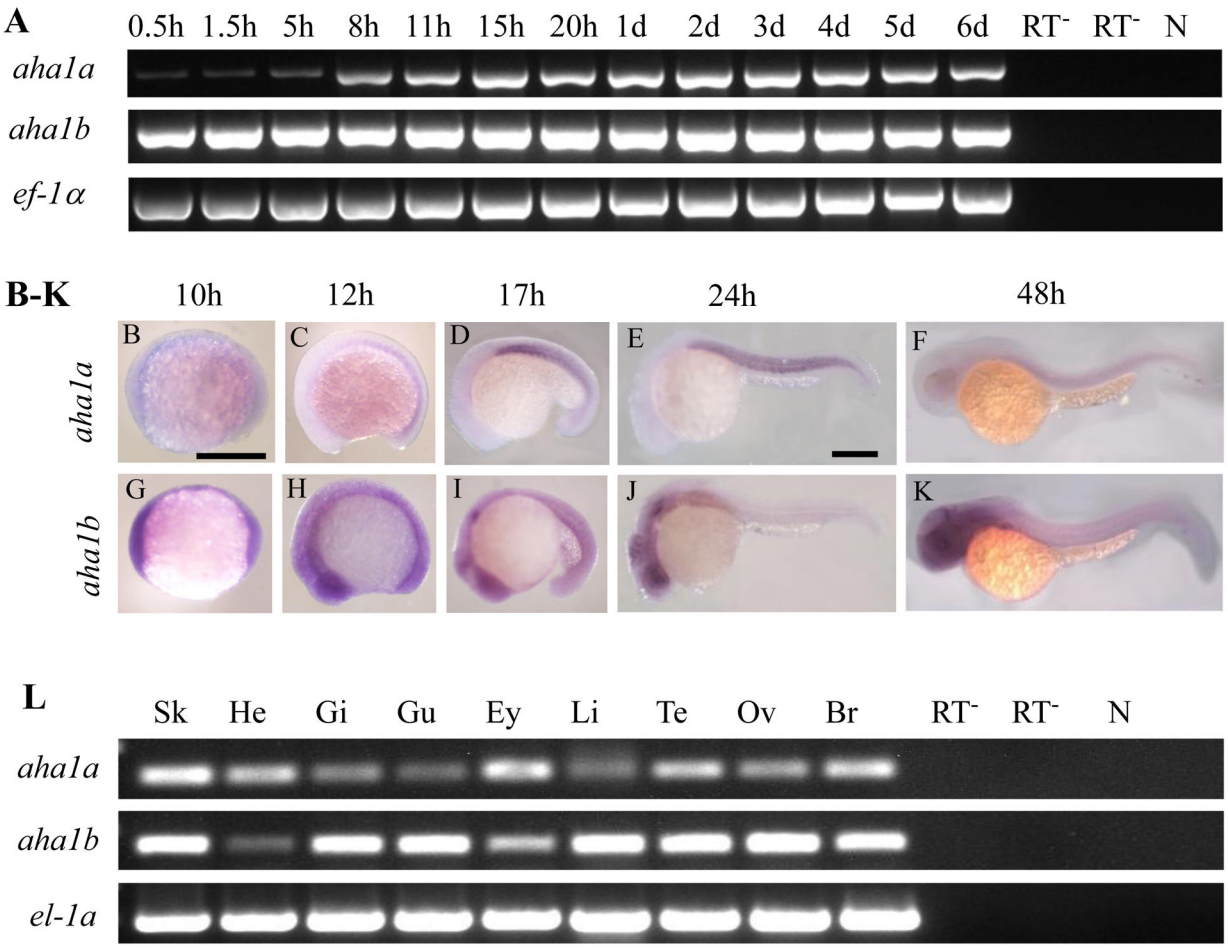

Figure 2. The temporal and spatial patterns of *aha1a* and *aha1b* gene expression in zebrafish (*Danio rerio*) embryos and various adult tissues.

A. RT-PCR shows the temporal expression of *aha1a* and *aha1b* genes during embryonic development at various stages from newly fertilized eggs to six days postfertilization (6 dpf) zebrafish larvae. EF1α was included as an internal reference control. Two RT- RNA samples from 5d and 6d and water (N) were included as negative controls. B-K. *In situ* hybridization shows the expression of *aha1a* and *aha1b* in zebrafish embryos during early embryogenesis (10 – 48 hpf). Approximately 30–40 embryos were analyzed for each gene at each stage. The expression of *aha1a* was restricted to developing somite and skeletal muscles (B-F) and *aha1b* was expressed broadly in the whole embryos with stronger signals in the head regions (G-K) before 48 hpf. Scale bars =150 μm. L. *aha1a* and *aha1b* are ubiquitously expressed in adult tissues including skeletal muscle (Sm), heat (He), gill (Gi), gut (gu), eyes (Ey), liver (Li), testes (Te), ovaries (Ov), and brain (Br). Primers for RT-PCR were designed at the junctions of two adjacent exons to eliminate potential problems with genomic DNA contamination. Two RT- RNA samples from ovaries and brain and water (N) were included as negative controls.

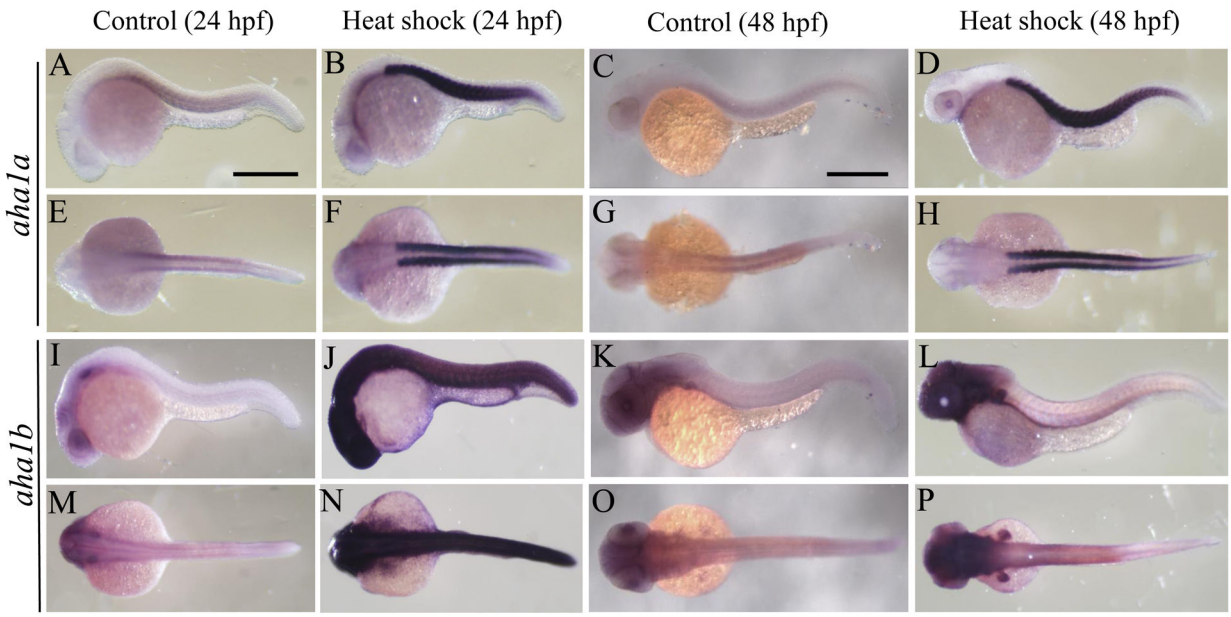

Figure 3. The effects of heat shock on *aha1a* and *aha1b* mRNA expression in wildtype zebrafish embryos.

Wild type zebrafish embryos (n=50) were heat shocked for 1 hr at 37°C at 24 hpf or 48 hpf, respectively. The heat shocked embryos and respective untreated controls were fixed and used for expression analysis of *aha1a* and *aha1b* mRNA transcripts by whole mount *in situ* hybridization. The data show *aha1a* expression in controls at 24 hpf (A, E) and 48 hpf (C, G) and heat shocked treated groups at 24 hpf (B, F) and 48 hpf (D, H), respectively. A strong muscle-specific upregulation of *aha1a* expression was observed in heat shock treated embryos at 24 and 48 hpf. The data show *aha1b* expression in controls at 24 hpf (I, M) and 48 hpf (K, O) and heat shocked treated groups at 24 hpf (J, N) and 48 hpf (I, I), respectively. A dramatic global upregulation of *aha1b* expression was observed in heat shock treated embryos at 24 hpf (J, N). The upregulation was more pronounced at the head region at 48 hpf. A-D and I-L are side views. E-H and M-P are dorsal views. Scale bars = 100 μm.

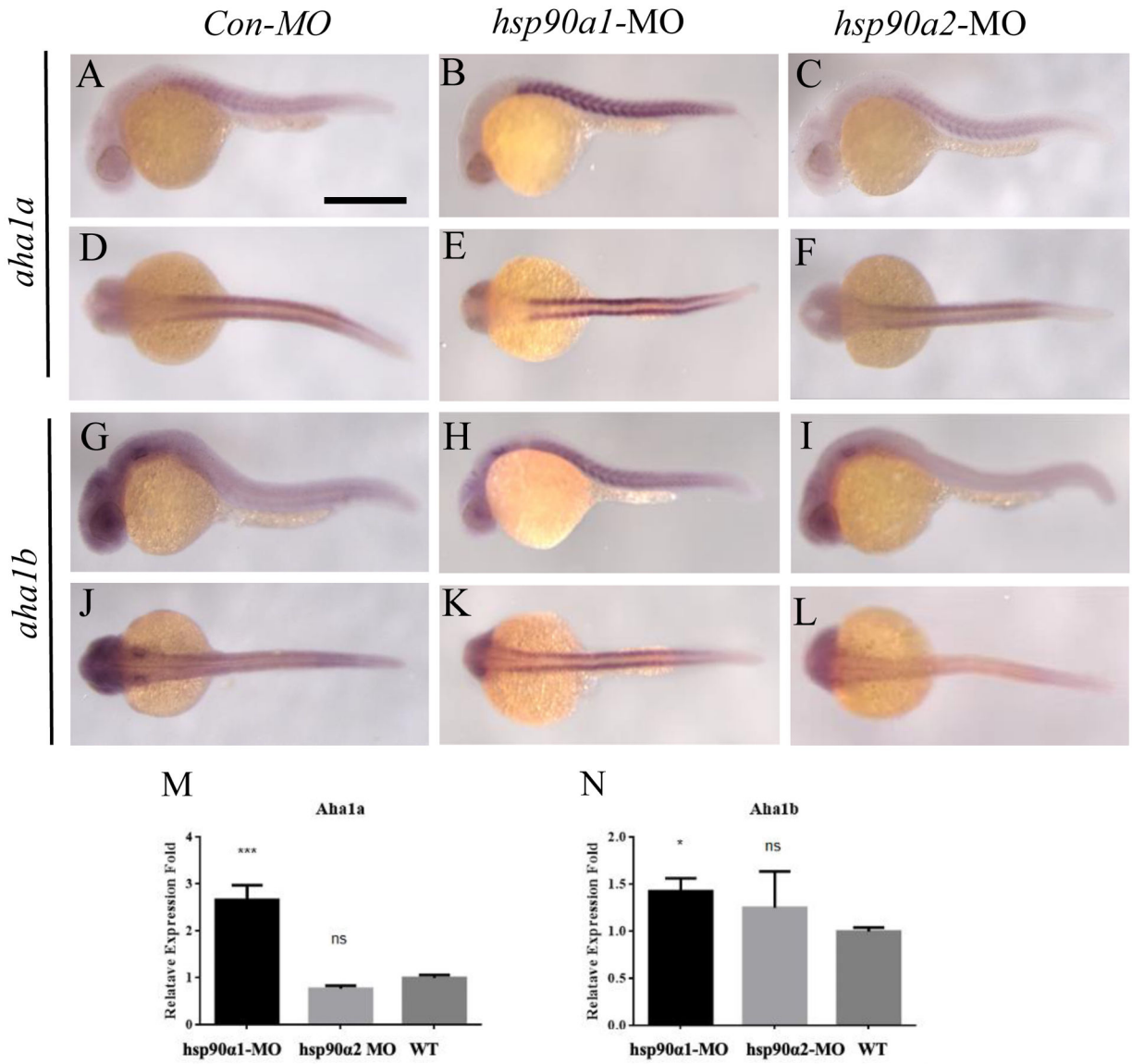

Figure 4. Upregulation of *aha1a* and *aha1b* expression in defective muscle of *hsp90a1* knockdown zebrafish embryos

Fertilized eggs were injected with control (Con-MO), *hsp90α1-MO* or *hsp90α2-MO* morpholinos at 1 or 2 cell stages. The *aha1a* and *aha1b* gene expression was analyzed by whole mount *in situ* hybridization and qRT-PCR in the injected embryos (n=120 for each MO) at 24 hpf. A-F, *aha1a* expression in Con-MO (A, D), *hsp90α1-MO* (B, E) and *hsp90α2-MO* (C, F) injected embryos, respectively. G-L, *aha1b* expression in Con-MO (G, J), *hsp90α1-MO* (H, K), and *hsp90α2-MO* (I, L) injected embryos, respectively. A-C, G-I: side views. D-F, J-L: dorsal views. Scale bar = 100 μm. M and N, qRT- qPCR analysis shows levels of *aha1a* (M) and *aha1b* (N) mRNA expression in *hsp90α1, hsp90α2*, and control embryos at 24 hfp.

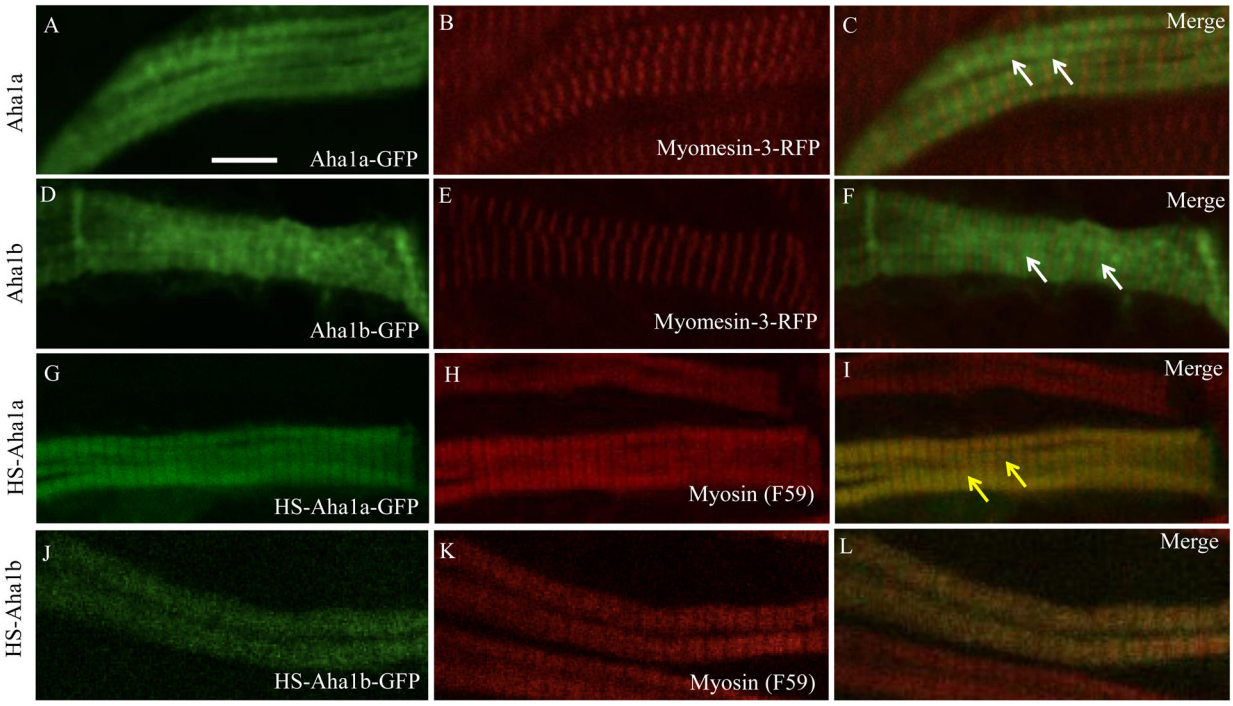

Fig. 5. Subcellular localization of Aha1a-GFP and Aha1b-GFP in myofibers of zebrafish embryos under normal and heat shock conditions.

DNA constructs expressing Aha1a-GFP or Aha1b-GFP fusion proteins were microinjected into zebrafish embryos. Each group of the injected embryos were randomly divided into two subgroups. One subgroup (~30 embryo) was subjected to heat shock (HS) treatment (37°C) for 1 hr at 48 hpf, another subgroup (~30 embryo) was used as untreated control. Subcellular localization of Aha1a-GFP and Aha1b-GFP was determined in myofibers of control and heat shock treated embryos together with M-line (Myomesin-3-RFP) and myosin (F59) markers. A-C, Confocal analysis shows Aha1a-GFP (A), Myomesin-3-RFP (B) and the merged (C) localization in myofibers of control embryos. D-F, Aha1b-GFP (D), Myomesin-3-RFP (E) and the merged (F) localization in myofibers of control embryos. G-I, Aha1a-GFP (G), myosin (F59, H) and the merged (I) localization in myofibers of heat shocked embryos. J-L, Aha1b-GFP (J), myosin (F59, K) and the merged (L) localization in myofibers of the heat shocked embryos. White arrows in (C) and (F) indicate sarcomeric Aha1a-GFP and Aha1b-GFP localization between the M-lines (Myomesin-3-RFP). Yellow arrows in (I) indicate the Aha1a-GFP colocalization with myosin (F59) in the A bands. Due to the mosaic pattern of gene expression via DNA injection, myofibers labeled with Myomesin and Myosin antibodies did not always express the aha1a-GFP or aha1b-GFP transgene. Scale bar = 6 μm.

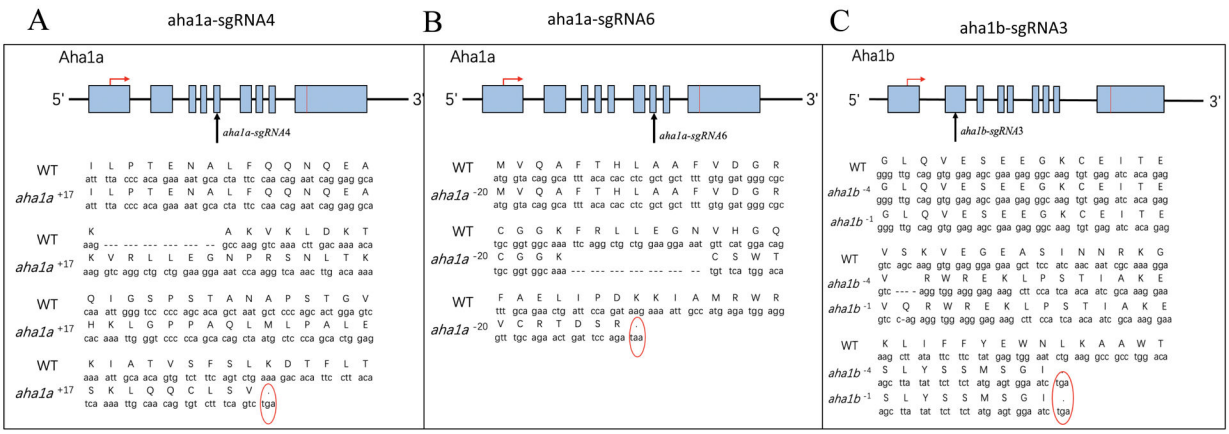

Figure 6. Generation of *aha1a* and *aha1b* zebrafish mutants using CRISPR/Cas9.

Gene specific sgRNAs targeted to *aha1a* or *aha1b* were co-injected with Cas9 protein into fertilized embryos at 1–2 cells stages. Two mutant alleles were generated for each gene. A and B, the $aha1a^{+17}$ and $aha1a^{-20}$ mutant alleles were generated using *aha1a-sgRNA-4* and *aha1a-sgRNA*- 6 targeted to *aha1a* gene exon 5 and 7, respectively. The $aha1a^{+17}$ and $aha1a^{-20}$ alleles carry a 17 bp insertion and 20 bp deletion, respectively. C, the $aha1b^{-1}$ and $aha1b^{-4}$ mutant alleles were generated using the same *aha1b-sgRNA-3* targeted to exon 2 of *aha1b* gene. The $aha1b^{-1}$ and $aha1b^{-4}$ alleles carry a 1 bp and 4 bp deletion, respectively. All these indel mutations created reading frame shift in *aha1a* or *aha1b*, resulting in premature stop codons in their coding sequences.

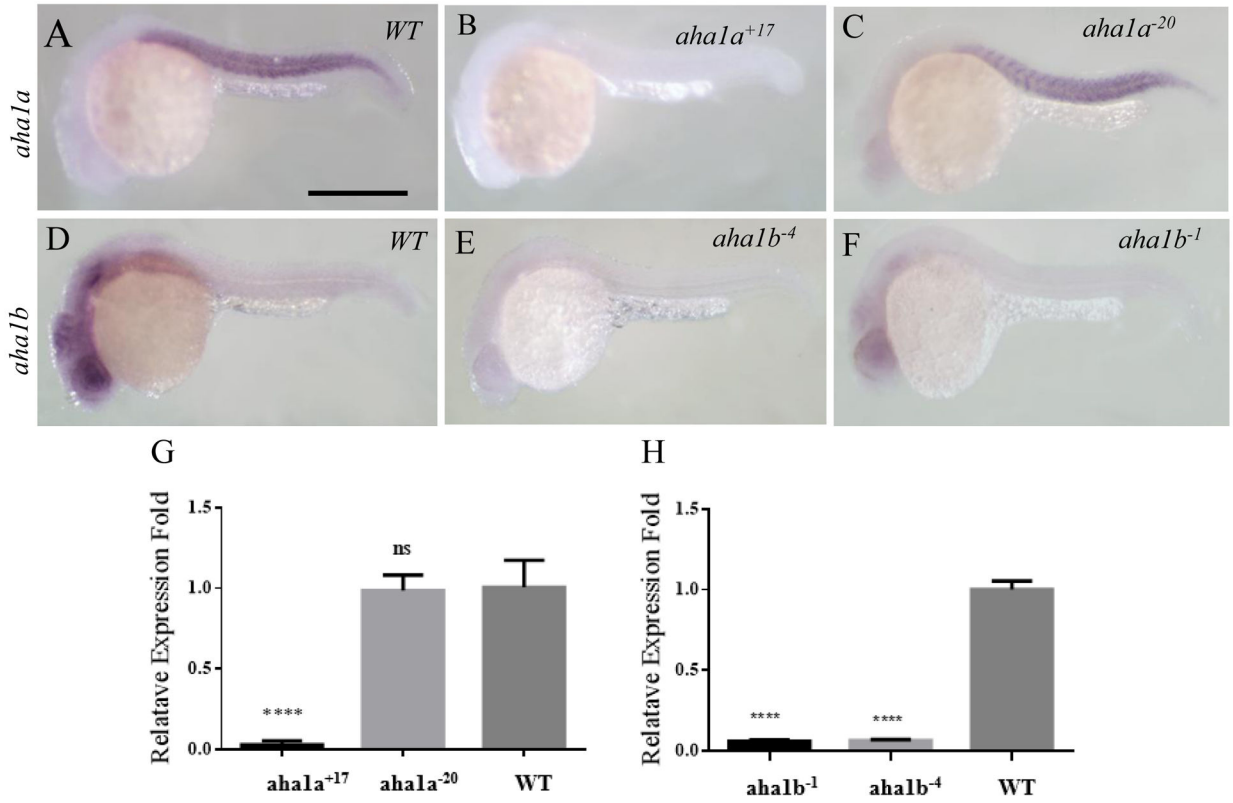

Figure 7. Comparison of *aha1a* and *aha1b* mRNA expression in WT, *aha1a* and *aha1b* mutant embryos.

aha1a and *aha1b* mRNA expression was analyzed by whole mount *in situ* hybridization (A-F) and qRT-PCR (G, H) in WT, *aha1a*$^{+17}$, *aha1a*$^{-20}$, *aha1b*$^{-4}$and *aha1b*$^{-1}$mutant embryos (approximately 30 embryos for each group) at 24 hpf. A-C, *aha1a* expression in WT control (A) and *aha1a*$^{+17}$ (B) *aha1a*$^{-20}$ (C) mutant embryos. D-F, *aha1b* expression in WT control (D), *aha1b*$^{-4}$(E) and *aha1b*$^{-1}$(F) mutant embryos. All pictures are side views. Scale bar = 100 μm. G and H, qRT-PCR analysis of *aha1a* and *aha1b* mRNA expression in WT control and *aha1a* (G) and *aha1b* (H) mutant zebrafish embryos at 24 hpf. Expression of *elongation factor 1-alpha (Ef-1 α)* was used an internal reference gene. Error bars are mean ± SEM. ***P<0.001 were considered statistically significant. Nonsense- mediated mRNA decay was detected in *aha1a*$^{+17}$, *aha1b*$^{-4}$and *aha1b*$^{-1}$mutant alleles.

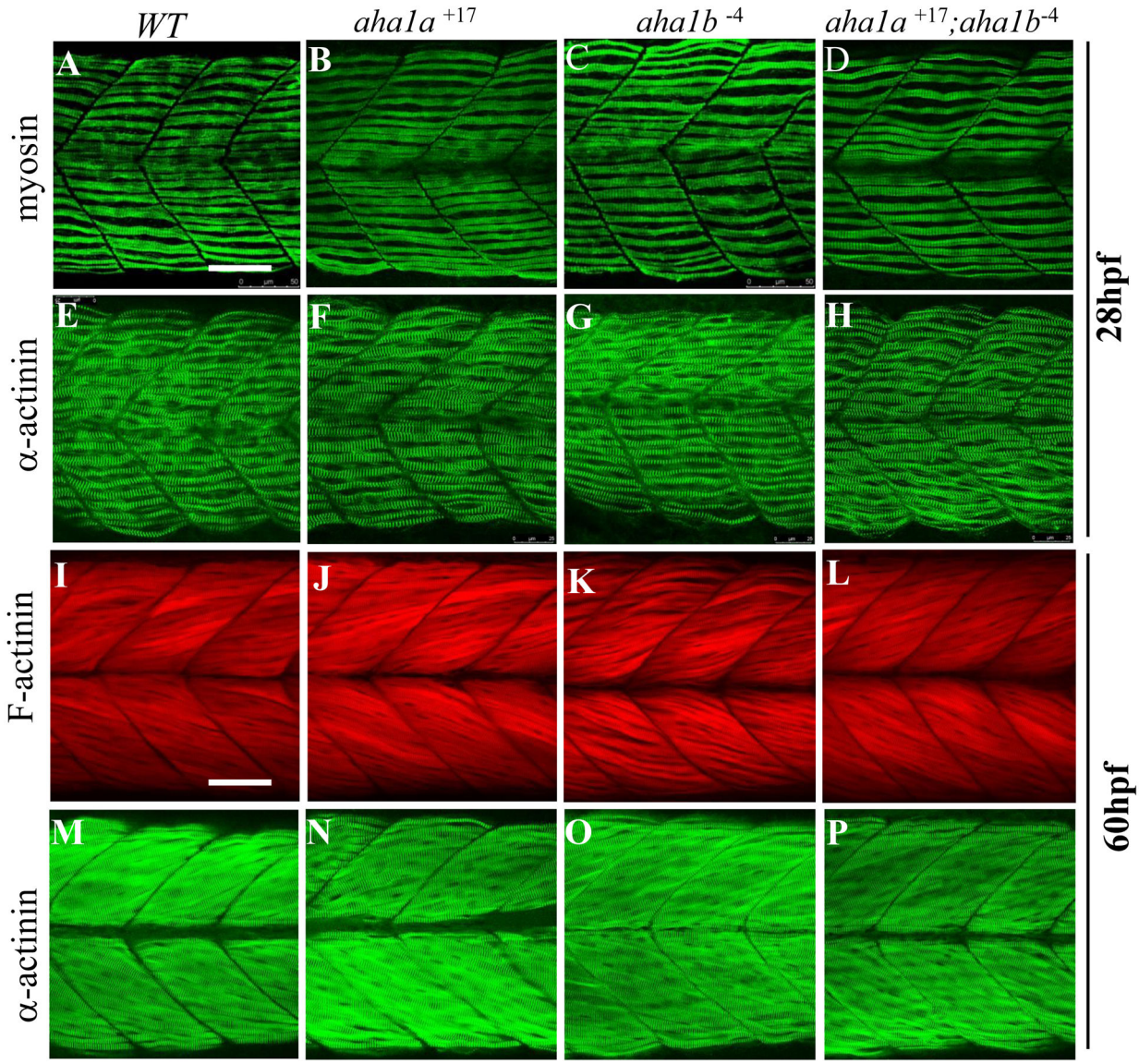

Figure 8. Characterization of muscle cell differentiation and sarcomere organization in slow and fast muscles of *aha1a* and *aha1b* mutant embryos.

Myofibers in slow and fast muscles of WT, *aha1a*$^{+17}$, *aha1b*$^{-4}$single and *aha1a*$^{+17}$; *aha1b*$^{-4}$ *double* mutant embryos (~80 fish embryos for each group) were analyzed by phalloidin and immunostaining that specifically label various sarcomere structures. A-D: Myosin organization in slow fibers revealed by F59 antibody staining of WT (A), *aha1a*$^{+17}$(B), *aha1b*$^{-4}$(C) and *aha1a*$^{+17}$; *aha1b*$^{-4}$(D) mutant embryos at 28 hpf. E-H: Z-line organization in slow fibers revealed by anti-α-actinin antibody staining of WT (E), *aha1a*$^{+17}$(F), *aha1b*$^{-4}$(G) and *aha1a*$^{+17}$; *aha1b*$^{-4}$(H) mutant embryos at 28 hpf. I-L: a-actin thin filament organization revealed by Phalloidin staining of WT (I), *aha1a*$^{+17}$(J), *aha1b*$^{-4}$(K) and *aha1a*$^{+17}$; *aha1b*$^{-4}$(L) mutant embryos at 60 hpf. M-P: Z-line organization in fast fibers shown by anti-α-actinin antibody staining in WT (M), *aha1a*$^{+17}$(N), *aha1b*$^{-4}$(O) and *aha1a*$^{+17}$; *aha1b*$^{-4}$(P) mutant embryos at 60 hpf. All pictures are side views of part of trunk muscles. Scale bar = 25 μm.

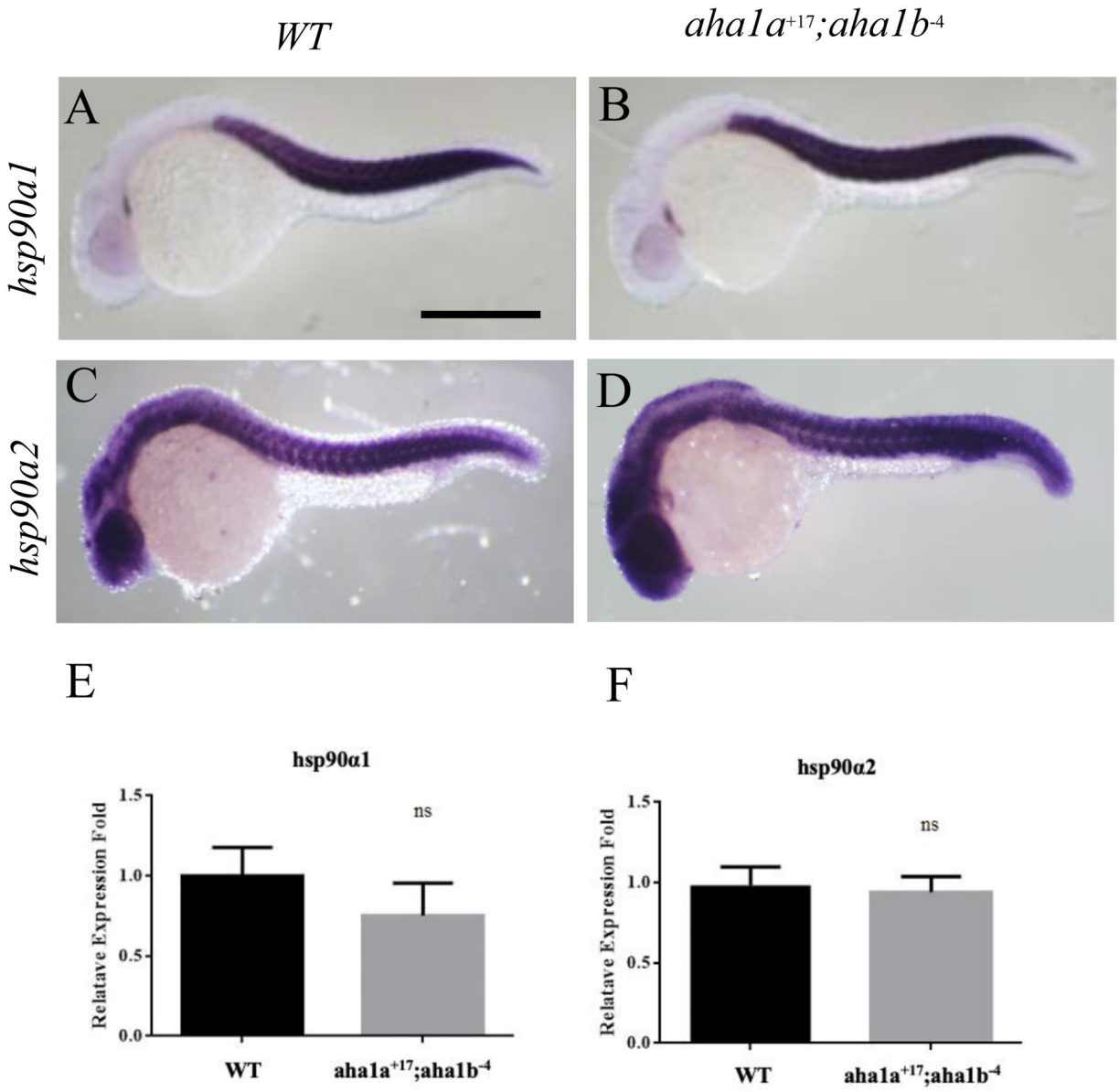

Figure 9. Knockout of *aha1a and aha1b* has no effect on *hsp90α1* and *hsp90α2* gene expression in fish embryos.

Expression of *hsp90a1* and *hsp90a2* was determined by whole mount *in situ* hybridization (A-D) and qRT-PCR (E, F) in WT control (A, C) and *aha1a*$^{+17}$; *aha1b*$^{-4}$double mutant (B, D) zebrafish embryos at 24hpf, respectively. WT embryos (n=51) and *aha1a*$^{+17}$; *aha1b*$^{-4}$double mutant embryos (n=50) were applied for *in situ* hybridization. Total RNA was extracted from zebrafish embryos (triplicates of 25 each) at 24 hpf in each group for qRT-PCR, respectively. All pictures here are side views. Scale bar = 100 μm.

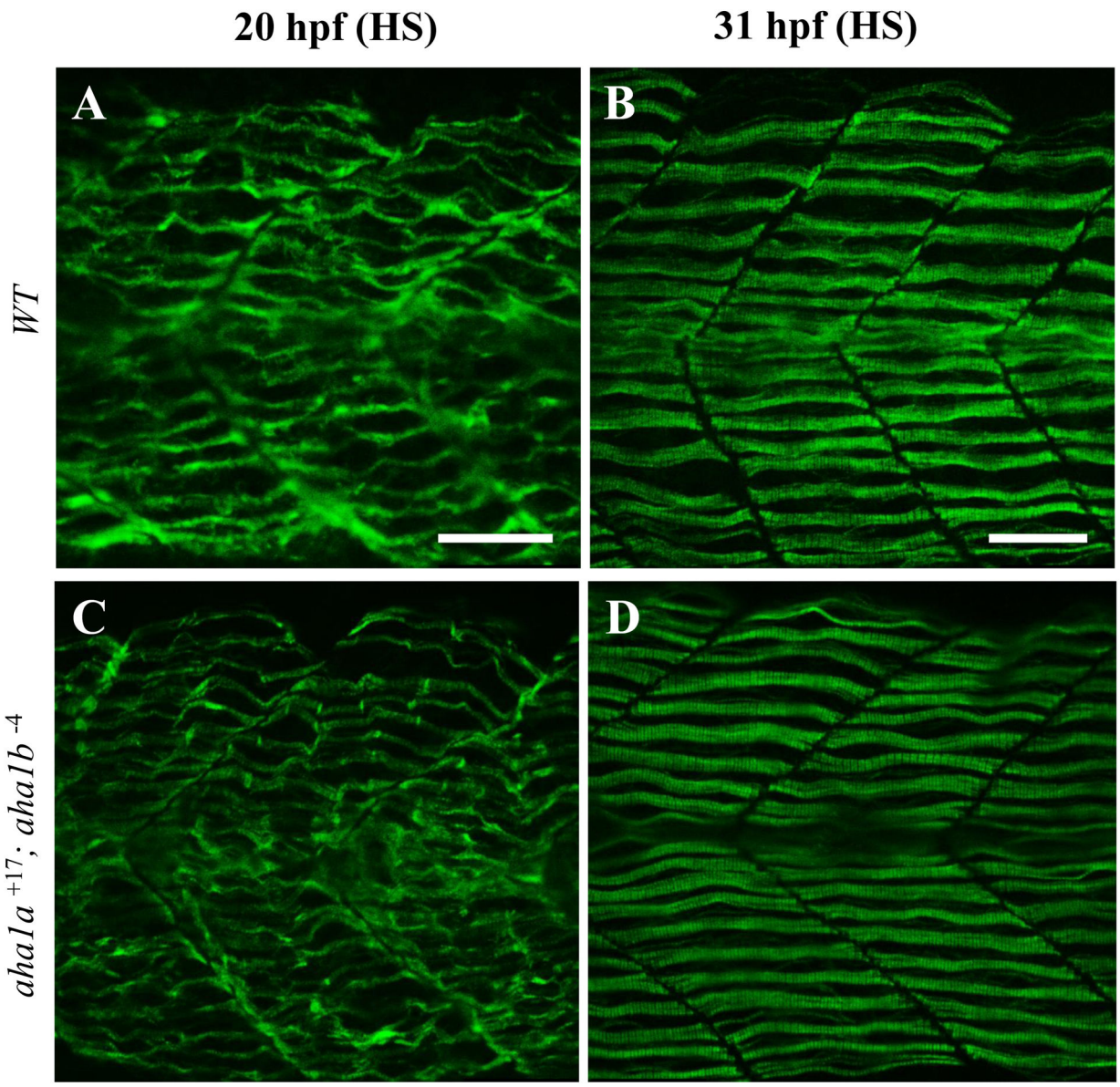

Figure 10. The effect of heat shock on muscle development in Aha1a and Aha1b double mutant embryos.

WT (n=50) and *aha1a*$^{+17}$; *aha1b*$^{-4}$double mutant (n=50) embryos were subjected to heat shock (HS) at 20 hpf or 31 hpf under 37°C for 1h. Muscle development in the treated embryos was analyzed by immunostaining with F59 antibody that showed myosin thick filament organization in WT (A, B) and *aha1a* and *aha1b* double mutant (C, D) embryos at 20 and 31 hpf, respectively. No significant difference was detected between WT and *aha1a*$^{+17}$; *aha1b*$^{-4}$mutant embryos. All pictures are side views of part of trunk muscles. Scale bar = 25 μm.

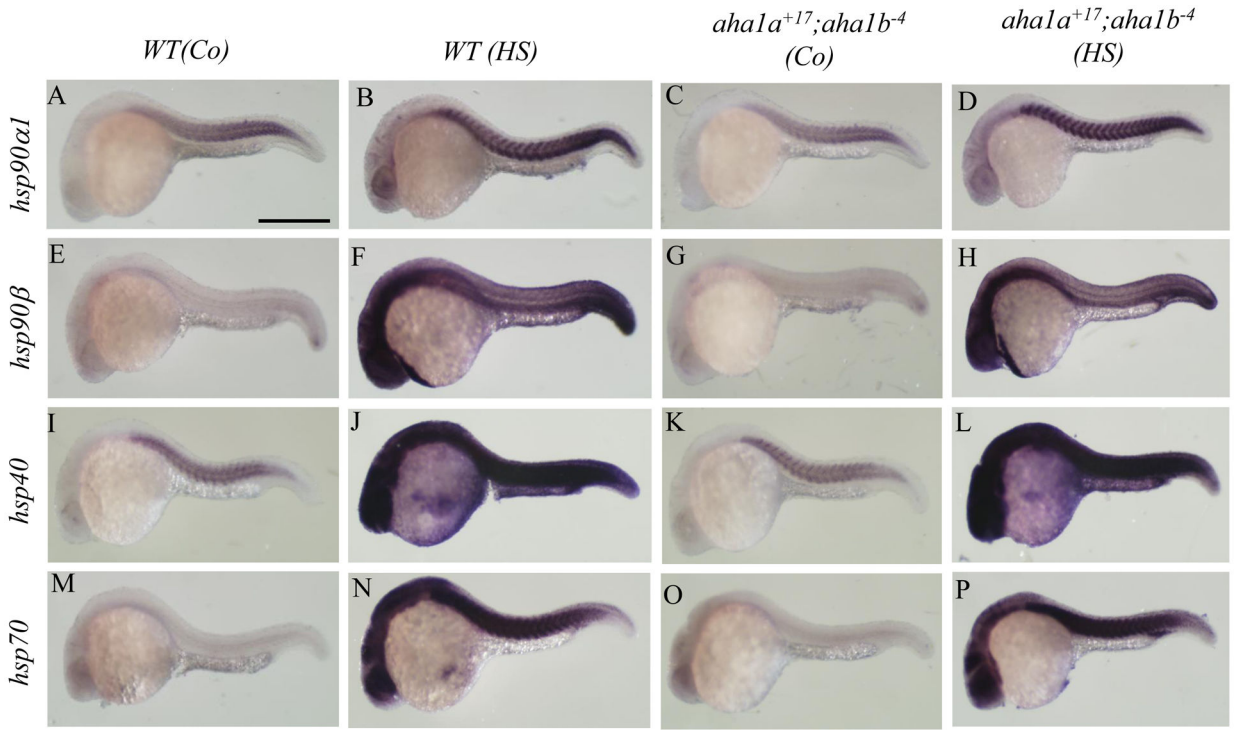

Figure 11. Heat shock response in *aha1a* and *aha1b* double mutant embryos.

WT (n=120) and *aha1a*$^{+17}$; *aha1b*$^{-4}$double mutant (n=120) embryos were subjected to heat shock (HS) at 24 hpf under 37°C for 1h. mRNA expression of *hsp90α1* (A-D), *hsp90β* (E-H), *hsp40* (I-L) and *hsp70* (M-P) were analyzed in untreated (A, E, I and M) and heat shock treated (B, F, J and N) WT control group as well as untreated (C, G, K and O) and heat shock treated (D, H, L and P) *aha1a*$^{+17}$; *aha1b*$^{-4}$ double mutant group. Comparable upregulation of *hsp90α1, hsp90β*, *hsp40*, and *hsp70* was observed in WT and *aha1a*$^{+17}$; *aha1b*$^{-4}$ mutant embryos. All pictures here are side views. Scale bar = 100 μm.

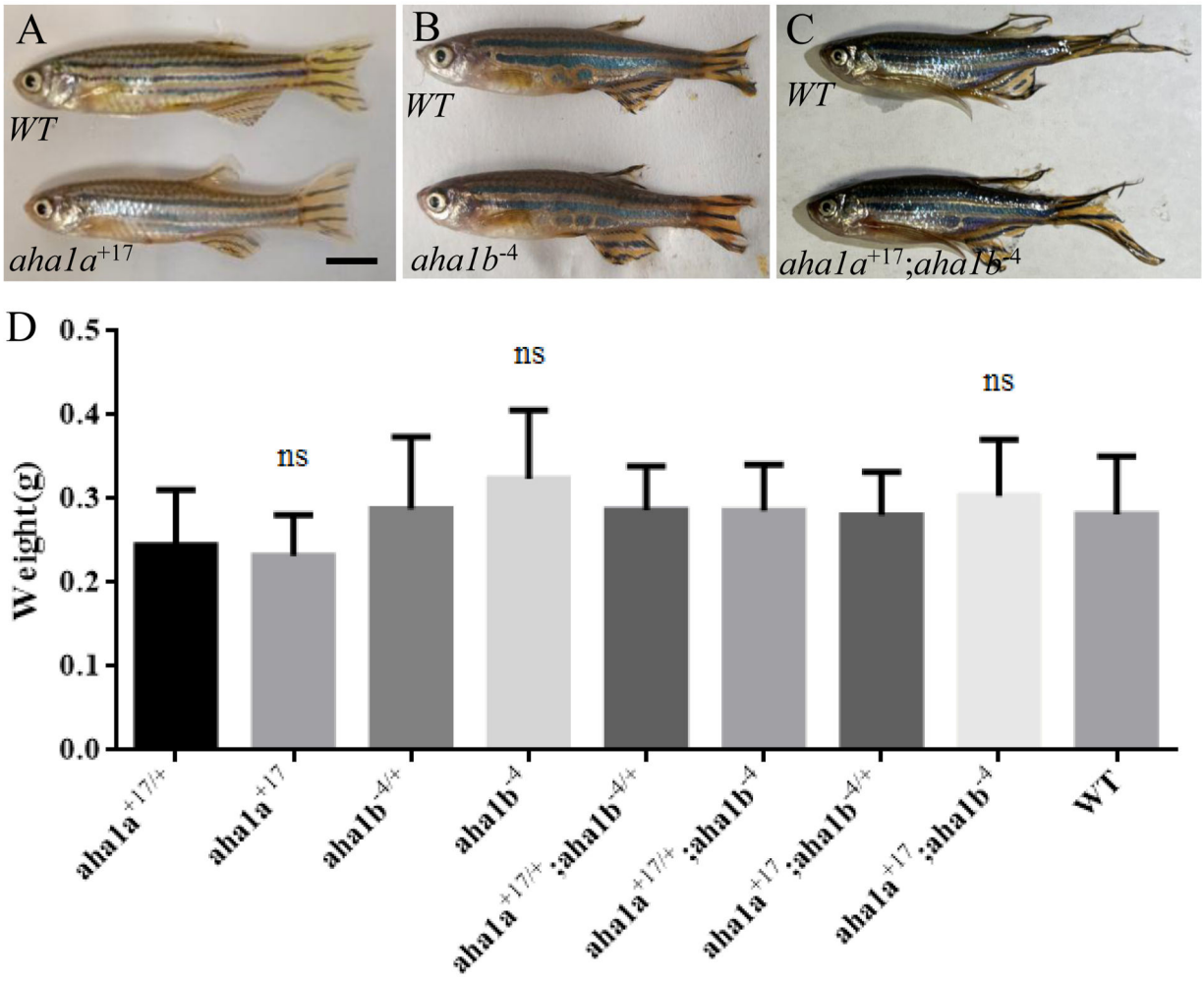

Figure 12. Knockout of *aha1a and aha1b* has no effects on fish growth and survival.

A-C. Morphological comparison among WT, *aha1a*$^{+17}$(A), *aha1b*$^{-4}$(B) and *aha1a*$^{+17}$; *aha1b*$^{-4}$(C) mutant fish at 10-month-old. D. Body weight (g) comparison among fish generated from in-cross of *aha1a*$^{+17/+}$, *aha1b*$^{-4/+}$ or *aha1a*$^{+17/+}$; *aha1b*$^{-4/+}$ double heterozygous mutants at 10-month-old. Adult fish (n=162) generated above were used for body weight testing. Scale bar = 1.3 cm. Weight differences among different genotypes of zebrafish were analyzed using a Student's t-test. No significant difference was detected in terms of body weight among these groups (P>0.05). Error bars are ± SEM.

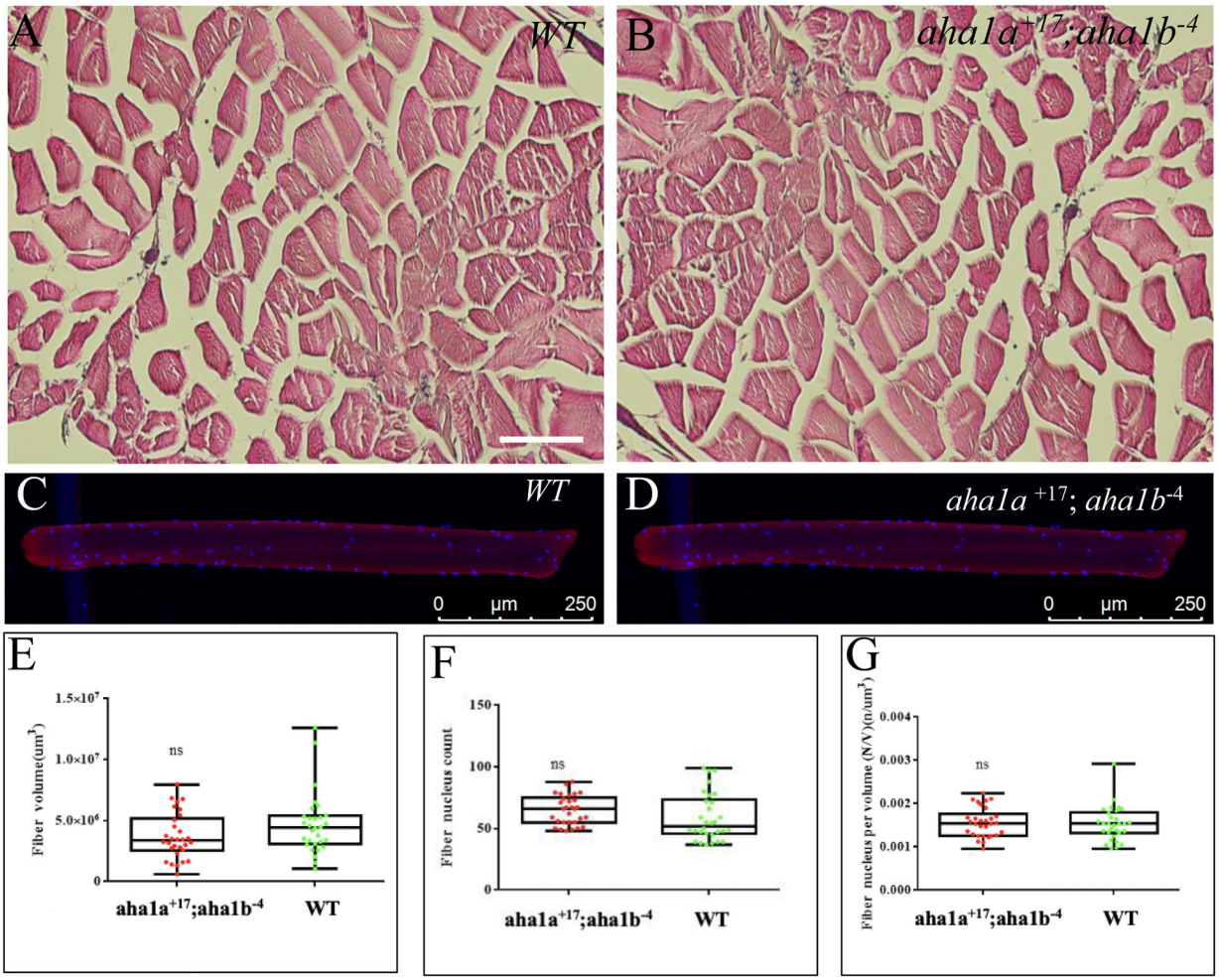

Figure 13. The Aha1a and Aha1b double mutants displayed normal muscle growth.

Skeletal muscles were dissected from three WT and three *aha1a*$^{+17}$; *aha1b*$^{-4}$double mutant fish at 5- month-old. A and B, Skeletal muscle structures were analyzed by haematoxylin and eosin (HE) staining in cross sections of trunk muscles from WT (A) and *aha1a*$^{+17}$; *aha1b*$^{-4}$double mutant (B), respectively. Scale bar = 50 μm. C and D, single myofibers were dissected from skeletal muscles of WT (C) and *aha1a*$^{+17}$; *aha1b*$^{-4}$double mutant (D) fish at 5-month-old. The dissected single fibers (n=35, each) were stained with Hoechst 32258 and Phalloidin-TRITC. Average myofiber volume (E), nuclear count (F) and per nuclear volume (G) were calculated and compared between WT and *aha1a*$^{+17}$; *aha1b*$^{-4}$double mutant. No significant difference was detected between WT and *aha1a*$^{+17}$; *aha1b*$^{-4}$mutant fish. Error bars are Median± SEM. Differences between WT and mutants were analyzed using a Student's t test